University of Tartu

Faculty of Science and Technology

Institute of Chemistry

Siiri Saaver

PRODRUG APPROACH FOR THE CELLULAR DELIVERY OF POLYANIONIC INHIBITORS OF PROTEIN KINASE CK2

Master's Thesis

Supervisor: Kaido Viht, PhD

Tartu 2014

Table of contents

Abbreviations

ACN – acetonitrile

AM – acetoxymethyl

ATP – adenosine 5'-triphosphate

BODIPY FL – 4,4-difluoro-5,7-dimethyl-4-bora-3a,4a-diaza-*s*-indacene-3-propionic acid

Boc – *tert*-butyloxycarbonyl

CAMK – calcium/calmodulin-dependent protein kinase

DCE – 1,2-dichloroethane

DIC – *N*,*N'*-diisopropylcarbodiimide

DIPEA – *N*,*N*-diisopropylethylamine

DMEM – Dulbecco's modified eagle medium

DMF – dimethylformamide

DMSO – dimethyl sulfoxide

DTT – dithiothreitol

EDTA – ethylenediaminetetraacetic acid

ESI-MS – electrospray ionization mass spectrometry

FA – fluorescence anisotropy

FBS – fetal bovine serum

Fmoc – fluorenylmethyloxycarbonyl

FRET – Förster resonance energy transfer

GTP – guanosine 5'-triphosphate

HBSS – Hank's Balanced Salt Solution

HBTU – *N,N,N',N'*-tetramethyl-*O*-(1*H*-benzotriazol-1-yl)uronium hexafluorophosphate

HeLa – cervical cancer cells derived from Henrietta Lacks

HEPES – 4-(2-hydroxyethyl)-1-piperazineethanesulfonic acid

HOBt – hydroxybenzotriazole

HPLC – high-performance liquid chromatography

HRMS – high-resolution mass spectrometry

IC_{50} – half-maximal inhibitory concentration

ICR – ion cyclotron resonance

K_d – equilibrium dissociation constant determined from a displacement assay

K_D – equilibrium dissociation constant determined from a direct binding assay

K_i – equilibrium dissociation constant determined from an inhibition assay

K_m – Michaelis constant

MS – mass spectrometry

Nala – *N*-methylglycine

Nasp – *N*-carboxymethylglycine

NHS – *N*-hydroxysuccinimide

Nlys – *N*-4-aminobutylglycine

NMM – *N*-methylmorpholine

NSG – *N*-substituted glycine oligomers

NTP – nucleoside triphosphate

PBS – phosphate-buffered saline

PNBP – 4-(4-nitrobenzyl)pyridine

RPMI – Roswell park memorial institute medium

SPPS – solid phase peptide synthesis

TBBi – 4,5,6,7-tetrabromo-1*H*-benzimidazole

TBBi-oca – 8-(4,5,6,7-tetrabromo-1*H*-benzimidazol-1-yl)octanoic acid

TFA – trifluoroacetic acid

TK – tyrosine kinase

TKL – tyrosine kinase-like

TIPS – triisopropylsilane

1. Introduction

Phosphorylation of proteins is one of the most important processes in living cells. Phosphorylation can induce signalling and change enzymatic activity. Enzymes, which catalyse the transfer of a phosphoryl group from nucleoside triphosphate (NTP) to protein, are called protein kinases.

CK2 is a unique protein kinase differing from other kinases in several aspects. CK2 has many substrates in a human organism and it accepts both ATP (adenosine triphosphate) and GTP (guanosine triphosphate) as a phosphoryl group donor. CK2 is active in the form of free catalytic subunit and as holoenzyme. It is acidophilic, meaning that it recognizes substrates that contain negatively charged amino acid residues around the phosphorylatable residue. The increased activity of CK2 is associated with many diseases, most frequently with cancer, which makes CK2 a target for pharmacy.

Asko Uri research group has developed bisubtrate ARC-type inhibitors with high affinity towards CK2. The compounds are negatively charged in physiological environment as they contain several aspartate residues.

A cell membrane is a negatively charged phospholipid bilayer therefore it allows the permeation of positively charged compounds and hydrophobic molecules. This complicates the introduction of compounds containing aspartate residues into cells. One possibility to lead highly charged compounds into cells is to mask the negative charges of the former, *e.g.* with the esterification of the carboxylates. This modification endows the compounds with cell membrane penetrative properties. Once the esterified compound is inside a cell, intracellular esterases cleave the ester groups and the compound will be trapped inside the cell in an active form.

The aim of this master's thesis was to synthesize a cell permeable esterase-activated CK2 bisubstrate inhibitor, determine its ability to penetrate the cell membrane and examine its intracellular stability.

2. Literature overview

2.1. Protein kinases

Protein kinases are enzymes that catalyse the transfer of phosphoryl group from nucleoside triphosphate (NTP) to a hydroxyl group of an amino acid residue in a protein (Figure 1). Phosphorylation causes alterations in the protein shape by adding several negative charges into the structure of the latter, which leads to development or loss of further interactions. The reaction in which a phosphate group is removed from the protein is called dephosphorylation and is regulated by enzymes called phosphatases. Thereby, protein kinases and phosphatases influence many mechanisms and reaction pathways through the regulation of phosphorylation equilibrium.

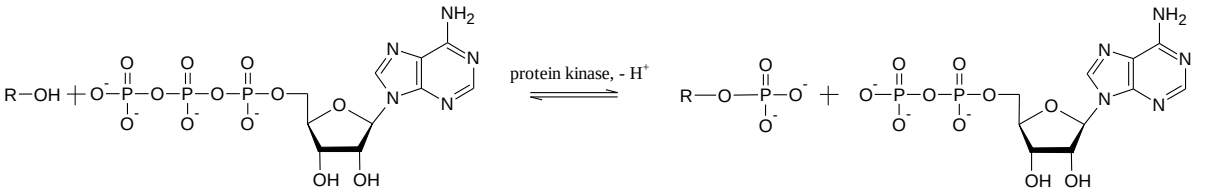

Figure 1. γ-phosphoryl group transfer from ATP to protein. R – Ser, Thr or Tyr residue.

The genes of over 500 known protein kinases make up about 2% of human genome [1]. Most of the protein kinases phosphorylate serine or threonine residues and ca 90 kinases are specialized in phosphorylation of tyrosine residues [1]. Additionally, there are a few dual-specificity kinases, which have the ability to phosphorylate both serine/threonine and tyrosine residues [2]. Most protein kinases use ATP as a phosphoryl group donor, but few kinases are able to utilize guanosine triphosphate (GTP) and other nucleotides on that purpose, although with a lower efficiency [3, 4].

Eukaryotic protein kinases are divided into groups, families and subfamilies based on amino acid sequence of the catalytic domain, biological functions and substrate specificities [5, 6]. Kinases in AGC group need to be activated by secondary messengers (cyclic nucleotides, phospholipids *etc*.) and they catalyse the transfer of phosphoryl group to the hydroxyl group of serine/threonine preferably near basic amino acid residues [7]. Calcium/calmodulin-dependent protein kinase (CAMK) group contains kinases that are regulated by Ca^{2+}/calmodulin [7]. In CMGC group, there are kinases that phosphorylate substrates rich in proline residues [7]. CK1 group was named after casein kinase 1 and it phosphorylates sequences containing many acidic residues [6]. STE group includes kinases that are involved in with activation of MAPK and related kinases [5]. Tyrosine kinase (TK) group kinases phosphorylate tyrosine residues and tyrosine kinase-like (TKL) kinases are

serine/threonine kinases structurally similar to TK kinases [5]. There are in addition atypical kinases, which have unusual structure, *e.g.* transmembrane receptors, with an intracellular kinase domain [6].

Protein kinases are essential biological catalysts, which strongly affect the life of cells by different mechanisms. They can be involved in enzyme activation and inactivation, protein localization, stabilization, degradation *etc*. The malfunction of protein kinases is associated with several serious diseases including cancer, which is the reason why protein kinases have become one of the targets of pharmacy. The activity of protein kinases can be suppressed with inhibitors. As of 2013, 26 small molecule inhibitors of protein kinases were approved for clinical use and several were in advanced clinical trials [8]. These inhibitors are mostly targeted at cancer, but also at rheumatoid arthritis and myelofibrosis. Altogether, about 50-70% of the current cancer targeted drug research are focused on inhibitors of protein kinases [8].

The majority of protein kinase inhibitors are targeted to the ATP binding site of the enzyme (Type I inhibitors). As ATP concentration in cells is in the millimolar range, it is relatively difficult for ATP competitive inhibitors to efficiently inhibit the kinase [9]. Another major drawback of ATP-competitive inhibitors is their low selectivity due to highly conserved ATP binding region in different kinases, which might result in possible side effects. Acquirement of selectivity for ATP competitive inhibitors is very challenging, although not impossible [9]. Sometimes lack of specificity is not a drawback, because it might enable to use the inhibitor against several PKs within the same pathway contributing to one disease [8]. Another class, Type II inhibitors, prevent the activation of PK by binding to an inactive form of the enzyme. Type II inhibitors have a better potency *in vivo* than Type I inhibitors, because ATP does not bind to the inactive conformation of the kinase. Bisubstrate inhibitors are active site targeted inhibitors, which consist of two fragments and each fragment binds to a targeted binding site. The advantage for competing with two substrates is the ability to create more interactions with the target enzyme and hence give a better inhibition potency and selectivity.

2.2. Protein kinase CK2

Protein kinase CK2, previously known as casein kinase 2, is a ubiquitous and constitutively active protein kinase, which is evolutionally highly conserved [10]. Two regulatory subunits β (26-42 kDa each) consolidate two catalytic subunits (α or α') into a heterotetrameric 140 kDa holoenzyme ($\alpha_2\beta_2$, $\alpha'_2\beta_2$, $\alpha\alpha'\beta_2$, Figure 2) [10-11]. Catalytic isoforms α (42-44 kDa) and α' (38 kDa) are structurally different to the extent of 25% of amino acid sequence, however their

activities do not vary significantly [10, 12]. CK2 catalytic subunits are active with or without the presence of β subunits, but the tetrameric structure of CK2 is more stable and its activity is generally even higher when compared to the free catalytic subunits [11, 13]. Both types of CK2 catalytic subunit are related to CMGC group kinases, but possess distinguishable sequences [10]. CK2 has many basic amino acid residues in its catalytic domain to interact with substrates containing several acidic amino acid residues [10]. No other kinases in CMGC group display such acidophilicity and unlike other CMGC group kinases, CK2 does not need to be phosphorylated to be maximally active [10]. Regulatory subunits influence the peptide substrate selectivity towards CK2; for example, CK2 holoenzyme does not phosphorylate calmodulin, whereas the catalytic α subunit does [14]. CK2β contains a zinc-binding motif called zinc-finger, which helps to create a highly stabilized holoenzyme once Zn^{2+} ions are bound [15]. The holoenzyme complex has a low nanomolar dissociation constant value and therefore displays high stability [13]. It is proposed that with the assistance of β subunits, supramolecular assembly of three holoenzymes is generated, which regulates the activity of CK2 [11].

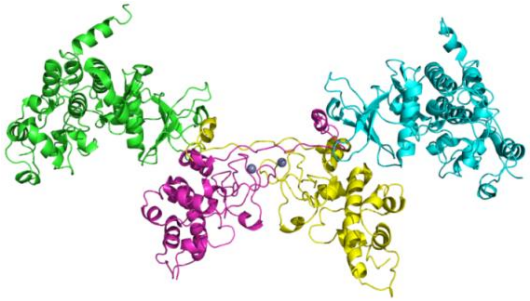

Figure 2. Holoenzyme of CK2. Green and blue domains depict α subunits, violet and yellow domains depict β subunits and grey spheres depict Zn^{2+} ions (PDB 4DGL).

CK2 is a pleiotropic kinase, which means it is able to transfer a phosphoryl group to many different substrates. It is proposed that about 20% of a human phosphoproteome is phosphorylated by CK2 [16]. The consensus sequence of phosphoacceptor sites of CK2 substrates is (E/D/x)-(S/T/Y)-(D/E/x')-(E/D/x)-(E/D)-(E/D/x), where S/T/Y is the acceptor of phosphoryl group, x is any residue except basic residues and x' additionally excludes proline residue [17]. The most important residue for efficient binding is at the position n+3, which is found in 90% of sites [17]. The second most important residue lies at position n+1 and is found in 75% of the sites. When an acidic residue is missing at the position n+3, then it is always at the position n+1 and *vice versa* [17]. Basic residues at positions between n-1 to n+4 are not well tolerated and have a negative effect on the affinity between the substrate and CK2 [17]. Phosphoserine can replace Glu and Asp residues in every position. On average, there are

over five negatively charged side chains in the phosphoacceptor site of a protein, which is phosphorylated by CK2 [17].

Like most protein kinases, CK2 transfers the phosphoryl group to a serine or threonine residue, but in addition, CK2 is also capable of phosphorylating tyrosine [18]. CK2 can efficiently utilize both ATP and GTP as a phosphoryl group donor [3, 10, 19]. The K_m value of CK2 for ATP (6-12 μM) is slightly lower than for GTP (9-21 μM) [19]. As a few hundred substrates of CK2 is known, the kinase is involved in many cellular processes such as protection against cellular stress, transcriptional control, cell cycle and neural functioning [20]. CK2 is found in most mammalian cells and furthermore, CK2 is present nearly everywhere inside a cell [21]. Many research groups have detected CK2 in plasma membrane, cytoplasm, mitochondria, endoplasmic reticulum, cytoskeleton, centrosomes and nucleus [21]. It is thought that the subcellular localisation of CK2 is a dynamic process and can be altered depending on the requirement for the kinase at specific sites inside a cell [21].

Involvement of CK2 in many diseases has been reported: increased activity of CK2 is observed in cancer cells but also in several neurodegenerative diseases like Parkinson's and Alzheimer, cardiovascular and inflammatory diseases, viral and parasite infections [20]. The excessive activity of the kinase correlates with its over-expression [20]. It is thought that CK2 is neither the direct cause nor the consequence of a neoplastic transformation, but it provides a suitable environment for cancer [22]. CK2 generates pro-survival signals in cancer cells, which are vital for malignant cells dependent on defective apoptosis [22]. As the transformed cell becomes addicted to high levels of CK2, the suppression of the kinase activity can lead to apoptosis of the cell [22].

In order to decrease the abnormally elevated activity of CK2, inhibitors targeting this kinase can be applied. An example of a potent type I CK2 inhibitor is CX-4945, which has recently completed the Phase I clinical trial and entered Phase II [23, 24]. CX-4945 is an orally bioavailable inhibitor with a K_i value of 0.38 nM (Figure 3) [25]. The inhibitor is very selective as only 7 kinases out of 238 tested were inhibited more than 90% at 500 nM concentration of CX-4945 [26]. The clinical trial proved that CX-4945 can be administered safely to humans [23]. During the drug administration, the stolid tumor stabilized for at least 16 weeks [23].

Other examples of type I CK2 inhibitors are polyhalogenated benzimidazole and benzotriazole derivatives, which have shown high affinity towards this kinase [20]. For example, 4,5,6,7-tetrabromo-1*H*-benzimidazole (TBBi) has a K_i value towards CK2 0.5 μM

(Figure 3) [27]. There are several other structures that are under development for CK2 inhibitors, which are based on the scaffolds of flavonoid, coumarin, anthraquinone, xanthenone *etc*. [20]. Because of constitutive activity of CK2, type II inhibitors for CK2 have not been reported. [20].

A) 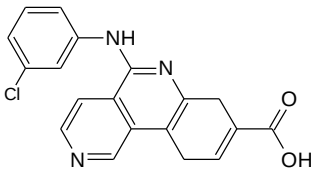

B) 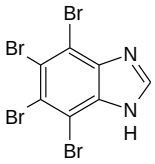

Figure 3. Structures of CX-4945 (**A**) and TBBi (**B**).

2.3. ARC-type inhibitors

ARC-type (previously abbreviated from *adenosine analogue oligoarginine conjugate*) inhibitors developed by Asko Uri research group are probably the most profoundly studied bisubstrate inhibitors of protein kinases [28]. ARCs are conjugates, where a fragment targeted at ATP binding cleft (usually aromatic heterocycle) and peptidic fragment are interconnected with a hydrophobic linker. ARC-type inhibitors are highly potent inhibitors with a great selectivity and the most potent compounds have their inhibition constants in the one-digit picomolar range [29].

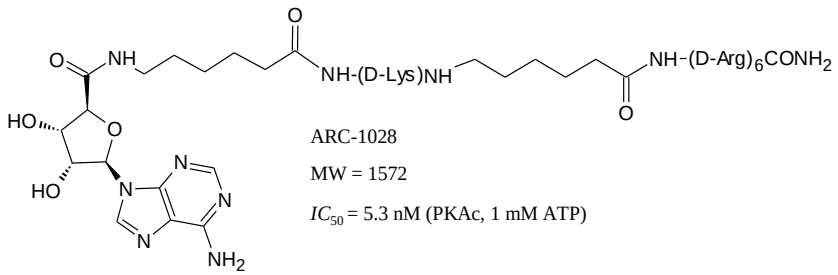

Figure 4. The third generation of ARC-type inhibitors [28].

The first generation of ARC-type inhibitors included adenosine and oligo-L-arginine attached *via* an aminohexanoic linker. The development of second generation ARCs included amidation of the C-terminus to remove the negative charge, which caused three- to fivefold increase in the inhibition potency [28]. The breakthrough in the development was the replacement of L-amino acids with D-amino acids, which increased the inhibition potency up to 100 times and also increased the proteolytic stability [28]. An extended linker with a chiral centre was inserted to the third generation of ARC-type inhibitors and this modification allowed a better binding between the inhibitor and the enzyme with a K_d value down to one-digit picomolar range (Figure 4) [29].

The specimens of the first generation of ARC-type inhibitors were successfully applied in cell experiments [30]. The oligoarginine constituent of an ARC-type inhibitor resembling a cell penetrating peptide promoted the conjugate to penetrate the plasma membrane, yet probably several different mechanisms of permeation were involved [30].

ARC-type inhibitors can be used as biosensors as they preserve high affinity even after tagged with a fluorescent marker [31]. Their affinity and selectivity can be adjusted by variation of their peptidic moiety, nucleosidic fragment or linker. Special type of ARC-type inhibitors incorporate thiophene or selenophene ring that after binding to a target kinase, produce a long lifetime photoluminescence signal upon excitement at near-UV region [32]. When a compatible fluorescent dye is attached to the probe, signal amplification occurs as a result of Förster resonance energy transfer (FRET) from the phosphorescence donor (thiophene or selenophene ring) to the fluorescent acceptor (fluorescent dye) [32]. This phenomenon is likely to occur with all protein kinases and it has great potential for real-time measurements of binding events in cells [32].

Recently, the bisubstrate inhibitor approach has been used for designing ARC-type inhibitors for CK2 [33]. Unlike ARCs targeted at basophilic kinases and containing an oligoarginine fragment, ARCs targeted at acidophilic CK2 contain negatively charged amino acids. Up to date the best disclosed bisubstrate inhibitor of CK2 is ARC-1502, which incorporates an oligoaspartate peptide, lysine residue for a dye attachment, octanoic acid linker and TBBi (Figure 5) [33]. The K_d value of ARC-1502 is in subnanomolar range (K_d = 0.52 nM), very similar to the K_d value of CX-4945 (K_d = 0.56 nM) [33]. The comparison of the affinities of ARC-1502 and its parent compound TBBi (K_i = 0.5 μM) towards CK2 shows clearly that ARC-1502 is much more potent CK2 inhibitor [27]. ARC-1502 is also more selective towards CK2 than TBBi, as only 10 kinases out of 140 in the selectivity panel were inhibited more than 50% while the residual activity of CK2 was 1% at 1 μM concentration of ARC-1502 [33]. The inhibition of several basophilic kinases such as Pim-1 and Pim-2 was observed with the parent compound TBBi, but not with ARC-1502, illustrating the high potential of bisubstrate approach for improving the selectivity of inhibition [33]. A fluorescent dye PromoFluor-647 was attached to ARC-1502 yielding a fluorescent ligand ARC-1504, which was demonstrated to be applicable in displacement assays to determine the affinities of non-labelled inhibitors of CK2 [33].

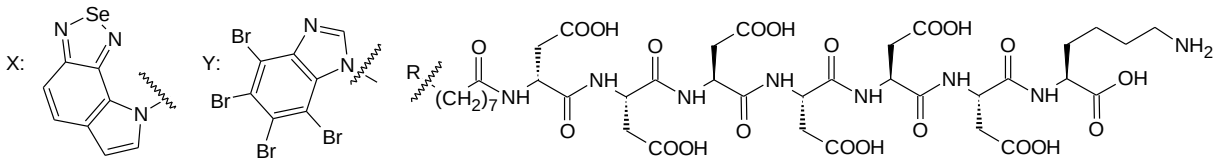

Figure 5. Structures of ARC-1502 (R = X) and ARC-3138 (R = Y).

Another ATP pocket-binding fragment benzoselenadiazole was introduced to yield a long-lifetime photoluminescent probe for CK2 [34]. ARC-3138 (K_d = 82 nM) emits luminescence in complex with CK2 while no long lifetime luminescence is emitted by the free ligand (Figure 5) [34].

2.4. Ester-loading technique for cellular delivery of anionic compounds

The plasma membrane consists of two layers of phospholipids and proteins embedded inside. It is a hydrophobic barrier that separates the interior of the cell from the exterior. Unfamiliar ionic and polar compounds are generally incapable of permeating the plasma membrane, while essential ions and other polar molecules can permeate the membrane by the aid of transporters. There are several techniques for the introduction of membrane impermeable compounds to cells such as electroporation, microinjection and cell penetrating peptide mediated cargo delivery.

A prodrug approach based on AM esters is often used to introduce negatively charged molecules inside cells [35-37]. These esters are membrane-permeable and they can be introduced to cell by simply applying the esters to extracellular medium [38]. Once inside the cell, acetyl group is on-ionic in esterase-catalyzed reaction and the hydroxymethyl ester is spontaneously cleaved releasing on-ioni and carboxylic acid (Figure 6). The molecule is incapable of leaving the cell resulting in increase of concentration of the compound inside cells [38]. The de-esterification is dependent on the concentration of the compound, time and temperature of incubation.

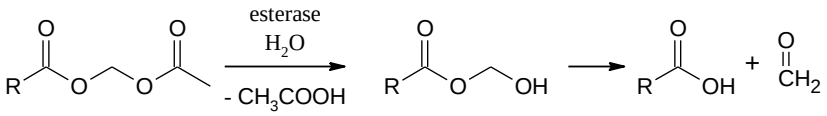

Figure 6. Hydrolysis of an AM ester.

Methanal and acetic acid are produced as side products, but their concentrations are low and therefore do not influence remarkably cellular processes [38]. This has been confirmed for several penicillin prodrugs (such as pivampicillin) that are acyloxymethyl esters (Figure 7) [39].

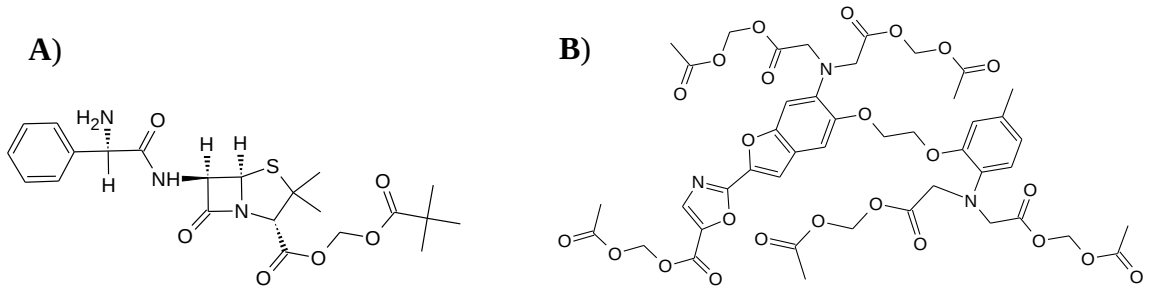

Figure 7. Structures of penicillin prodrug pivampicillin (**A**) and Fura-2 AM ester (**B**) [39].

As masking with AM esters changes the esterified compound more hydrophobic, the aqueous solubility of the compounds is decreased and the stock solutions of the compounds are usually made in dimethyl sulfoxide (DMSO) [40]. Additionally, surfactants like Pluronic F-127, which is a on-ionic dispersing agent, are frequently used to aid the dispersion of compounds containing AM esters in aqueous solutions to prevent precipitation [40].

Probably one of the most widespread fields of AM ester application is reducing the polarity of calcium indicators for cell internalization [40]. Fura-2 is a fluorescent dye that changes its absorption spectrum when bound to calcium (Figure 7) [40]. For cell permeation its five carboxylates are masked with AM esters [40].

Compared to more invasive techniques like electroporation and microinjection, the prodrug approach is a milder technique to introduce polar compounds to cells. A disadvantage of using AM esters for plasma membrane permeation of a compound is the incomplete hydrolysis of ester bonds [41]. The possible reasons for the incomplete de-esterification can be low activities of esterases and different rate constants for hydrolysis of AM esters at different positions. Another disadvantage of using AM esters is the possibility of accumulation in organelles [41]. A problem observed during the application of Fura-2 is the leakage of the compound out of the cells due to action of anion transporters. The leakage can be suppressed by anion transport inhibitors [41].

2.5. Solid-phase peptide synthesis (SPPS)

SPPS is the most widespread strategy for peptide synthesis. The synthesis is carried out on an insoluble polymer, e.g. cross-linked polystyrene resin [42]. The resin contains functional groups, which are the reaction centres for the first step of the synthesis. A resin loading is the amount of functional groups per mass unit of the resin.

Synthesis usually starts from the attachment of the most C-terminal amino acid residue of the peptide of interest and is carried out in repeated cycles (Figure 8) [43]. Each amino acid addition requires two steps: deprotection of N-terminal amino acid and attachment of the new

amino acid to the N-terminal of the peptide. Every amino acid is added in excess in order to accelerate the reaction and to enhance the yield. In order to remove the reagent surplus, resin is washed after every amino acid attachment.

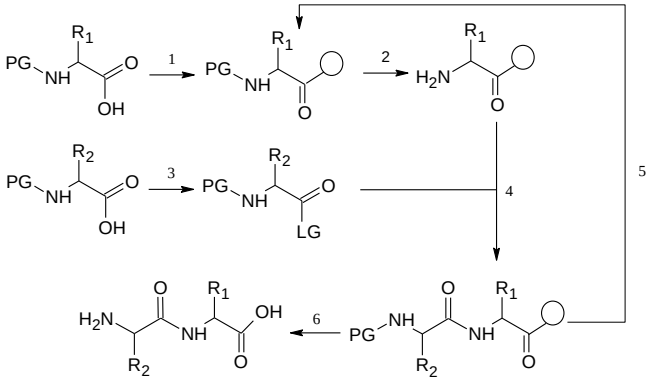

Figure 8. SPPS. PG – protection group, LG – leaving group 1) Attachment of the first amino acid to the resin. 2) Removal of the protection group PG from the α-amine. 3) Activation of the protected amino acid. 4) The formation of peptide bond. 5) Steps 2 two 4 are repeated until the desired peptide sequence is obtained. 6) Removal of the protection groups and peptide cleavage from resin.

After the attachment of the last amino acid, all protection groups are removed and the peptide is cleaved from the resin. Although peptide synthesis methods are highly optimized, longer peptides are difficult to synthesize using SPPS, as the yield of an amino acid attachment is never 100%. The side products attached to the resin cumulate and as they cannot be removed, they can drastically affect the final yield. Also longer peptide chains start to aggregate In the course of the synthesis.

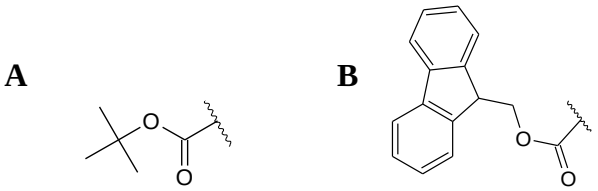

Figure 9. Boc (**A**) and Fmoc (**B**) protection groups.

The most utilized protecting groups of the α-amino group are *tert*-butyloxycarbonyl (Boc) and fluorenylmethyloxycarbonyl (Fmoc) (Figure 9) [44]. Boc is acid-labile and can be removed with trifluoroacetic acid (TFA) [43]. Fmoc is base-labile and can be removed with piperidine solution in dimethylformamide (DMF) [43]. The protection groups of the N-terminus and side chains must be orthogonal to avoid side reactions and for that combination for example Fmoc and *tert*-butyl ester can be used [43]. As *N*-acylation (for the formation of peptide bond) is an endergonic reaction, the carboxylic group needs to be activated. Coupling reagents, which form anhydrides and active esters, are used as activators (Figure 10) [44].

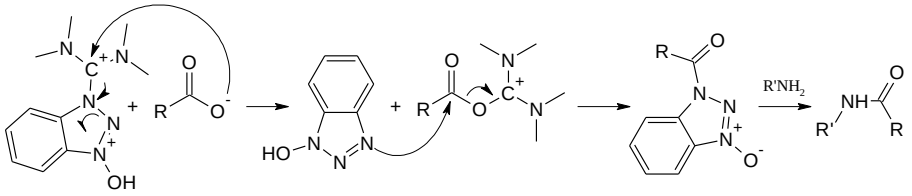

Figure 10. The proposed mechanism of carboxyl group activation with *N,N,N′,N′*-tetramethyl-O-(1*H*-benzotriazol-1-yl)uronium hexafluorophosphate (HBTU).

Nevertheless, SPPS does have its own shortcomings, such as large reagent consumption. The progression of the synthesis is difficult to observe, as the analysis of a peptide on a resin is complicated. Spectroscopic analyses are not as simple as in the case of liquid phase synthesis, because the products are not dissolved in the medium and the resin might also contribute to the detected signal. Chromatographic analyses are time consuming, because the product cleavage from the resin has to be done in advance.

In order to verify the presence of specific functional groups simple colour tests are applied, such as Kaiser test, which is used for detection of primary amines and thereby monitoring the completeness of the reaction [45]. The test is based on the reaction of ninhydrin with primary amino group, which yields a characteristic blue colour [45].

2.5.1. Aspartimide formation

The synthesis of aspartate- or glutamate-containing peptides can be problematic as an acid- or base-catalysed side reaction might occur that yields in a mixture of two peptides (Figure 11) [44]. In strong acid the side-chain ester is protonated and vulnerable to the attack by the amide nitrogen, whereas in the presence of base catalysis, the amide nitrogen is deprotonated, which induces an attack at the side-chain carbonyl group [44]. The rearrangement occurs through a cyclic imide intermediate and an aspartyl residue is more affected than a glutamyl residue [44]. The hydrolysis of the aspartimide yields in the formation of two structural isomers, α and β peptide, which have identical mass. Racemization in α-carbon can also occur during the formation of aspartimide.

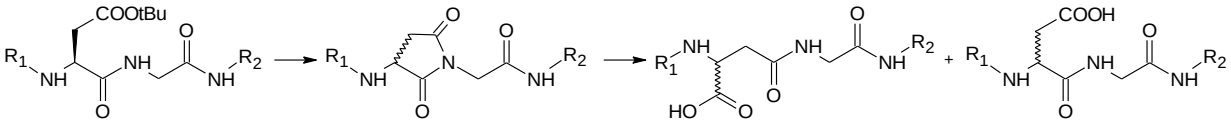

Figure 11. Evolvement of α and β peptides as the result of aspartimide formation.

The formation of aspartimide can be suppressed by adding a solution of HOBt at 0.1 M concentration in the deprotecting solution (20% piperidine in DMF) [44]. Aspartimides also

form during the esterification of aspartates in a peptide. It has been shown that aspartimide formation during esterification can be avoided by highly optimizing the synthesis [37].

2.6. Peptoids

Peptoids are *N*-substituted glycine oligomers (NSG), which makes them structural isomers of peptides (Figure 12) [46]. The side chain in peptoids is attached to an amide nitrogen instead of the α-carbon and thus the backbone of peptoids is achiral. No hydrogen bonds can form between the backbones of two peptoid chains, because a tertiary amide can act as a hydrogen bond acceptor, but not as a hydrogen bond donor. Due to structural differences it can be challenging to "translate" a peptide into a peptoid. Compared to peptides NSGs have distinct secondary structure, which has different electronic and steric interactions [47]. Like peptides are peptoids capable of forming helical secondary structure, although if the side chain of a peptoid is achiral, the formed helix is not very stable as it interchanges between α and β helix conformations. Although, when a peptoid includes α-chiral side chains and some aromatic side chains, then the formed α-helix is even more stable than the corresponding α-helix of a peptide [47-49]. The peptoid concentration, solvent and temperature have much less impact on the stability on peptoid helicity than for peptide helicity [47].

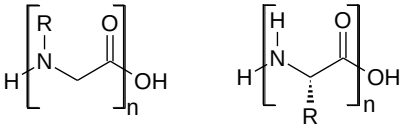

Peptoid Peptide

Figure 12. General structures of a peptoid and a peptide.

Peptoids have many promising therapeutic properties. NSGs are more resistant to enzymatic degradation as compared to α-peptides [50]. Their ability to permeate the cell membrane is also larger as they contain fewer hydrogen bonds and are therefore more hydrophobic [51].

Peptoids can be synthesized easily with many derivatization possibilities. There are different kinds of methods for peptoid synthesis [46].

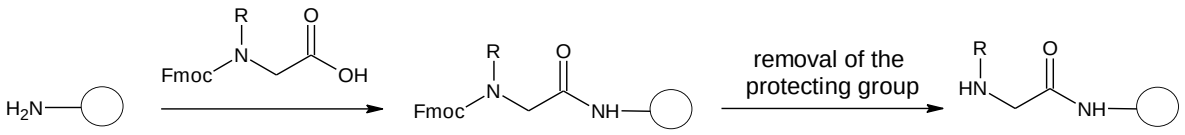

Figure 13. Monomer method of peptoids synthesis.

The first developed method is similar to the solid phase synthesis of peptides. Previously prepared *N*-Fmoc protected *N*-substituted glycine monomer is activated and attached to the secondary amino group of a peptoid chain, which is in turn attached to a resin bead (Figure

13) [46]. The Fmoc group is removed and the attachment of the next monomer follows [46]. A disadvantage of the method is the requirement of preparing the necessary *N*-substituted glycine monomers, which are either expensive or are not commercially available.

The most utilized synthesis method of peptoids is the submonomer method, which is based on alternating acylating and alkylating steps (Figure 14) [46]. An amine on a resin bead is acylated by an activated carboxylic acid derivative (often bromoacetic acid) [46]. During the acylation step the possible side-reaction is *N*-alkylation of resin bound amine with bromoacetic acid. However due to the difference in reaction rates this side reaction is insignificant [46]. The acylation reaction is 1000 times faster than alkylation and therefore only acylation is observed [46]. Acylation is followed by *N*-alkylation, where the halide (often bromide) is replaced with an amine [46]. As different primary amines have diverse reactivity, usually a high concentration of amine (typically 5-50 eq of amine at 0.3-2 M concentration) is used to guarantee the completeness of the reaction [46]. A typical cycle time for one monomer addition is about 150-180 minutes [46].

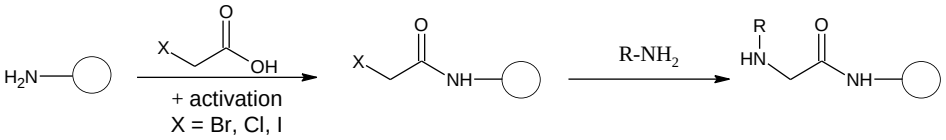

Figure 14. Submonomer method of peptoid synthesis.

While Wang resin is one of the most utilized resins for C-terminal carboxylate peptide synthesis, its application in peptoid synthesis is complicated, because a diketopiperazine formation prevents further chain extension (Figure 15).

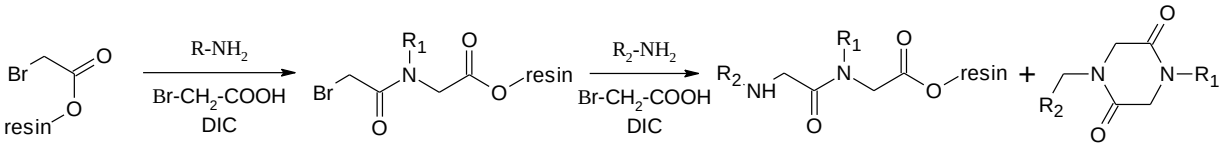

Figure 15. A diketopiperazine formation as a by-product.

The utilization of 2-chlorotrityl chloride resin has been shown to enable the synthesis of peptoids containing a free C-terminal carboxylate by preventing the formation of diketopiperazine by steric hindrance of the trityl group (Figure 16) [52].

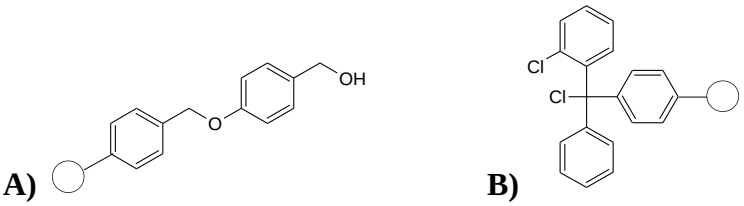

Figure 16. Structures of **A**) Wang resin **B**) 2-chlorotrityl chloride resin.

3. Experimental

3.1. Reagents and equipment

DMF was purchased from Acros Organics. Dithiothreitol (DTT), *N*-methylmorpholine (NMM), diethyl ether, bromomethyl acetate, *N*,*N*-diisopropylethylamine (DIPEA), Triton-X, *N*-Boc-1,4-butanediamine, 4-(2-hydroxyethyl)-1-piperazineethanesulfonic acid (HEPES), Tween 20, Pluronic F-127, DMSO, acetonitrile (ACN) were purchased from Sigma Aldrich. Fmoc-Gly-Wang resin, Fmoc-D-Asp(tBu)-Wang resin, 2-chlorotrityl chloride resin, HBTU and glycine *tert*-butyl ester hydrochloride were purchased from Iris Biotech. HOBt was purchased from Bachem. Fmoc-D-Asp(tBu)-OH and Fmoc-Sar-OH were purchased from NovaBiochem. Piperidine and triisopropylsilane (TIPS) were purchased from Alfa Aesar. Isopropanol was purchased from Rathburn. 1,2-dichloroethane (DCE), bromoacetic acid, triethylamine and *N*,*N'*-diisopropylcarbodiimide (DIC) were purchased from Fluka. TFA was purchased from Fischer Scientific. BODIPY FL C_5 *N*-hydroxysuccinimide (NHS) ester and cell-lysis buffer NP40 were purchased from Invitrogen. High glucose Dulbecco's Modified Eagle Medium (DMEM), Roswell park memorial institute medium (RPMI), Dulbecco's Phosphate-Buffered Saline (PBS), Hank's Balanced Salt Solution (HBSS), streptomycin, trypsin-ethylenediaminetetraacetic acid (trypsin-EDTA) solution and penicillin were purchased from PAA Laboratories. Sodium chloride was purchased from Riedel-de Haën and trypan blue from Bio-Rad. 8-(4,5,6,7-tetrabromo-1*H*-benzimidazol-1-yl)octanoic acid (TBBi-oca), ARC-1506, ARC-1507, ARC-1508, ARC-1509, ARC-1513o were synthesized by Jürgen Vahter. Human cervical cancer cells (HeLa, derived from Henrietta Lacks in 1951) were a kind gift from Beatson Institute for Cancer Research, Glasgow. The maintenance and seeding of cells was performed by Darja Lavõgina. $CK2\alpha^{1\text{-}335}$ (active human recombinant) was a kind gift from Olaf-Georg Issinger from Institute for Biochemistry and Molecular Biology, University of Southern Denmark.

Purification of the compounds was performed with Schimadzu LC Solution (Prominence) system by using manual injector, a diode array (SPD M20A) detector and a Shimadzu fluorescence detector (RF-$10A_{XL}$). Separation was achieved with a Gemini C18 5 µm column (250×4.6 mm i.d, Phenomenex) protected by a 5 µm Gemini C18 4×2.0 mm guard column. The ARC-1837 decomposition experiments were performed with a Luna C18 5µm column (250×4.6 mm i.d, Phenomenex) protected by a 5µm Luna C18 4×3.0 mm guard column. Mobile phase A: 0.1 % TFA, mobile phase B: 0.1% TFA in ACN and a flow of 1 mL/min were employed. Linear gradient elution was started at 3 min (injection time was also at

3 min). Electrospray ionization mass spectrometry (ESI-MS) mass spectra were measured in positive ion mode on Schimadzu LCMS-2020. ESI high-resolution mass spectrometry (HRMS) mass spectra were measured in positive ion mode on Thermo Electron LTQ Orbitrap on commercial basis at the Institute of Technology (University of Tartu). ICR-HRMS mass spectra were measured in positive ion mode on Varian 930 FT-ICR-MS by Tõiv Haljasorg. Purification of the compounds with high-performance liquid chromatography (HPLC) and ESI-MS analysis of compounds ARC-1801, ARC-1802, ARC-1803, ARC-1804, ARC-1805 and ARC-1806 were made by Gerda Raidaru.

The concentrations of the ligands were determined spectrophotometrically on a Nanodrop 2000c (Thermo Scientific) spectrophotometer. UV spectra were measured in a 2 μL volume with the optical path length of 0.1 cm. The following molar excitation coefficients were used: ε_{270nm}(TBBi-containing compounds) = 10 000 $M^{-1}cm^{-1}$, ε_{505nm}(ARC-1837) = 80 000, ε_{653nm}(ARC-1504) = 250 000 $M^{-1}cm^{-1}$, ε_{653nm}(ARC-1513o) = 150 000 $M^{-1}cm^{-1}$.

Fluorescence anisotropy (FA) was measured on a PHERAstar platereader (BMG Labtech) with a FA optical module [ex 590 (50) nm, em 675 (50) nm] using ARC-1504 and with a FA optical module [ex 540 (20) nm, em 590 (20) nm] using ARC-1513o. The solutions were prepared on 384-well microplates with non-binding surface (Corning) using Eppendorf Research (Eppendorf) pipettes and 8 channel 125 μL Voyager pipette (Integra).

Cell experiments were performed in an 8-well microscopy chamber (Ibidi). The viability of the cells was determined with a cell counter TC-10^{TM} (Bio-Rad). Cells were imaged with a microscope (TILL Photonics) using an oligochrome with xenon lamp and FITC filter [ex 475 (35) nm, em 525 (45) nm]. Images obtained with the microscope were analysed with ImageJ software (version 1.47).

Graphpad Prism software (version 5.00.288, GraphPad) and Microsoft Excel 2010 was used for data analysis.

3.2. Methods

3.2.1. Solid phase synthesis of peptides

Peptide fragments were synthesized with traditional Fmoc SPPS method on Wang resin. After every amino acid attachment, an aliquot of the resin was transferred to another synthesis vessel to vary the number of amino acids in the conjugates. Resin (initially 58 μmol, 90.8 mg) was swelled for 45 minutes in DMF. Protected amino acids (3 eq) were dissolved in DMF and activated with a mixture of HBTU/HOBt (2.94 eq each) and NMM (9 eq) in DMF. After

3 minutes of preactivation, the coupling solution was added to the resin (about 1 mL/100 mg of resin) and shaken for 40–60 min at room temperature. The completion of each coupling reaction was monitored with Kaiser-test. Fmoc-group removal was performed with double treatment of the resin with 20% piperidine solution in DMF (5+15 min). For the synthesis of ARC-1818, ARC-1819, ARC-1820, Wang resin (41.6 mg, 25.0 μmol was used and the Fmoc removal solution contained in addition 0.1 M HOBt. After each synthetic step the resin was washed five times. The coupling of TBBi-oca to peptides was carried out with 1.5 eq of the acid activated with HOBt/HBTU (1.47 eq each) in DMF/NMM and the reaction mixture was shaken for at least 3h. Finally the resin was washed 5 times with each solvent (DMF, isopropanol, DCE) and dried in vacuum. Treatment with TFA/H_2O/TIPS (90/5/5 by volume) for 2–3 h was used as the standard cleavage procedure. All the products were precipitated by the addition of 10 times excess volume of diethyl ether, pelleted by centrifugation and purified with HPLC using a gradient of 30%-90% ACN/30min followed by lyophilization. At least 300 nmol of every product was received. The structures of the compounds were confirmed by ESI-MS or ICR-HRMS mass-spectra (Appendices 2-12).

3.2.2. Solid-phase synthesis of peptoids

The peptoid parts of ligands were synthesized using a submonomer approach. After every monomer attachment, an aliquot of the resin was transferred to another synthesis vessel to vary the number of carboxylates in the conjugates. Loading (1.1 mmol/g) provided by resin producer was used. 2-chlorotrityl chloride resin (62.4 mg, 68.7 μmol,) was swelled for 1 hour in DMF. The first bromoacetic acid (5 eq) was attached to the resin dissolved in DCE with DIPEA (5 eq) for 2 hours at 40 °C. Washing with DCE and DMF (3 times both) followed. The consecutive bromoacetylations (5 eq bromoacetic acid) took place for 30 minutes in DMF at 40 °C with the assistance of DIC (5.5 eq).The primary amine (20 eq) was attached to the resin with a 2 hour reaction at 40 °C with the aid of DIPEA (20 or 40 eq). After every step resin was washed with DMF 5 times and the completion of every submonomer attachment was monitored with either chloranil test or PNBP test. The conditions of the TBBi-oca attachment and the cleavage of the compound were carried out as described above. All products were lyophilized and purified with HPLC using a gradient of 30%-90% ACN/30min. At least 300 nmol of every product was received. The structures of the compounds were confirmed with ESI-MS or ICR-HRMS (Appendices 2, 13-17, 20).

3.2.3. Fluorescence marker attachment

For the synthesis of ARC-1836, a solution of BODIPY FL C_5 NHS (1.5 eq) and triethylamine (50 eq) in DMF was added to ARC-1832. The reaction was stirred for 6 hours and then evaporated to dryness. The product ARC-1836 was purified with HPLC using a gradient of 30-90% ACN/30 min and the structure was confirmed with ESI-HRMS spectra (Appendices 2, 18).

3.2.4. Synthesis of AM esters

A solution of bromomethyl acetate (4.4 eq) and DIPEA (10 eq) in DMF was added to ARC-1836. The reaction was stirred overnight at room temperature. The product ARC-1837 was purified by HPLC with ACN/0.1% TFA gradient 40-90% ACN/25 min and confirmed by ESI-HRMS (Appendices 2, 19). The rest of the chromatographic peaks were analyzed with ESI-MS using external calibration. Peak 1 R_t = 17.9 min, $[M+H^+]^+$ found: 1352. Peak 2 R_t = 19.6 min, $[M+H^+]^+$: found: 1424. Peak 3 R_t = 21.3 min, $[M+H^+]^+$ found: 1497. Peak 4 R_t = 23.0 min, $[M+H^+]^+$: found: 1568. Peak 5 R_t = 24.6 min, $[M+H^+]^+$: found: 1640.

3.2.5. Determination of concentrations of ARC compounds

The concentrations of the solutions of ARC-compounds were determined using UV-Vis spectroscopy using molar extinction coefficients derived from literature. The absorption of the compound was measured in reference to the solvent used for dissolving the compound.

The concentration of the compound was calculated using Lambert-Beer law (Equation 1).

$$A = \varepsilon c l$$

Equation 1. Lambert-Beer law. A – absorption, ε – molar extinction coefficient, c – concentration, l – path length.

3.2.6. Fluorescence anisotropy assay

Fluorescence anisotropy assays were performed in the assay buffer (50 mM HEPES pH=7.5, 150 mM NaCl, 0.005% Tween 20, 5 mM DTT) with a final volume of 20 µL. Microplates were incubated for 10 or 20 minutes at 30 °C before the measurement.

A binding assay was used to determine the active concentration of $CK2\alpha^{1-335}$ by titrating the kinase with ARC-1504 [38]. A dilution series of $CK2\alpha^{1-335}$ starting from 200 nM (2-fold dilutions) was prepared and ARC-1504 was added to each well at fixed concentration (final total concentration of 10 nM). After the incubation, the values of fluorescence anisotropy were measured using 10 nM ARC-1504 solution without the kinase to calibrate the detector.

A graph was constructed with the kinase concentration on the horizontal axis and the anisotropy value on the vertical axis. The active concentration of CK2α$^{1\text{-}335}$ was calculated using non-linear regression analysis (Equation 2) [31].

$$Z = \frac{L_t + K_d + kx - \sqrt{(L_t + K_d + kx)^2 - 4L_t kx}}{2L_t}$$

$$M = \frac{QZ}{1 + Z(Q - 1)}$$

$$Y = (1 - M)A_f + MA_b$$

Equation 2. k – active/total kinase concentration, Y – measured anisotropy value, K_D – dissociation constant of the kinase and the ligand, L_t – total concentration of the ligand, x – total concentration of the kinase, Q – ratio of fluorescence intensities of bound and free ligand, A_b – anisotropy of completely bound ligand, A_f – anisotropy of the free ligand.

A displacement assay was used to determine the binding affinities of ligands. Fixed concentration of the fluorescent probe ARC-1504 (2 or 3 nM) or ARC-1513o (1 nM) in complex with the kinase CK2α$^{1\text{-}335}$ (3 or 2 nM) was added to each well of the concentration series of competing compound under interest (3 fold dilutions starting from 100, 10 or 1 μM).

$$e = (10^x - R_t)K_{d1} + (L_t - R_t)K_{d2} + K_{d1}K_{d2}$$

$$d = K_{d1} + K_{d2} + 10^x + L_t - R_t$$

$$f = -K_{d1}K_{d2}R_t$$

$$w = arccos\left[\frac{-2d^3 + 9de - 27f}{2\sqrt{(d^2 - 3e)^3}}\right]$$

$$j = 2\sqrt{d^2 - 3e}cos\frac{w}{3} - d$$

$$M = \frac{j}{3K_{d1} + j}$$

$$Y = (1 - M)A_f + MA_b$$

Equation 3. A_f – anisotropy of free fluorescence ligand; A_b – anisotropy of the complex; L_t – total concentration of the fluorescence ligand; R_t – total concentration of the active kinase; K_{d1} – dissociation constant between the fluorescence ligand and the kinase; K_{d2} – dissociation constant between the competing ligand and the kinase; x – logarithm of the total concentration of the competing ligand; Y – measured anisotropy value.

A solution with no inhibitor was prepared as the maximum reference value. After the incubation, the values of fluorescence anisotropy were measured using a 10 nM ARC-1504 solution without the kinase to calibrate the detector. The fluorescence anisotropy values were

analysed using exact competitive binding model (Equation 3) [31]. The anisotropy change is presented in reference to the solution containing no kinase. At least three parallel measurements were performed with freshly prepared solutions on different days.

3.2.7. Monitoring ARC-1837 decomposition

The qualitative analysis of the ARC-1837 decomposition in live cells and in buffer was determined with HPLC using a gradient of 30%-90% ACN/30min.

An HPLC analysis was conducted using DMSO solution of ARC-1837 (concentration of 2.1 mM) that had been stored at -20 °C for 1 month. A solution of ARC-1837 (10 μM) was made from the same stock solution in the buffer (50 mM HEPES pH=7.5, 150 mM NaCl, 0.005% Tween 20, 0.1% Pluronic F-127) and incubated at 37 °C for 24 hours. The hydrolysis reaction was monitored with HPLC at fixed time points (1.5; 3; 24 h). To determine the mass spectra of the decomposition products, ARC-1837 was dissolved in 50:50 DMSO:buffer (50 mM HEPES pH=7.5, 150 mM NaCl, 0.005% Tween 20) solution and incubated at 70 °C for 4 hours (Appendix 21). Non-decomposed ARC-1837 was used as an internal standard prior to HPLC analysis.

For intracellular decomposition analysis, cells were seeded on a 6-well culture plates at an initial density of 300 000 cells per well. Cells were grown in the medium (DMEM supplemented with 10% FBS, 100 U/mL penicillin, 100 μg/mL streptomycin) and maintained at 37 °C in a humidified 5% CO_2 environment for 2 days. After two days, the medium was removed and cells were washed with PBS twice. 10 μM ARC-1837 solution was prepared in serum- and antibiotics-free DMEM medium (500 μL) containing 1% DMSO and 0.1% Pluronic F-127. A control solution containing the same components but no ARC-1837 was also prepared. The solutions were added to cells and incubated for 1 h at 37 °C in humidified 5% CO_2 environment. Next, the solutions were removed and cells were washed twice with PBS. To cleave the proteins that bind cells to the plate, 400 μL of 0.25% trypsin-EDTA solution in PBS was added to both wells and the cells were incubated for 3 minutes. 3 mL of medium containing serum was used to wash cells off the plate surface and the suspensions were transferred to plastic tubes. The suspensions were centrifuged for 5 minutes at 100 g and the supernatants were removed. 1 mL of PBS was added to the pellets to wash the cells and the suspensions were centrifuged again with the same conditions. Next, the supernatants were removed and cells were thoroughly re-suspended with 1 mL of PBS. 15 μL of both cell suspensions were taken for cell viability experiments. The rest of the cell suspensions (each ca 985 μL) were centrifuged at 100 g for 5 minutes, the supernatants were removed and the

pellets were re-suspended in 200 μL of cell lysis buffer with 1% Triton-X. Cells were lysed on ice for 30 minutes with mixing after every 10 minutes. For protein precipitation, 400 μL of ACN was added to both of the samples and the solutions were mixed for 3 minutes. Next, the solutions were centrifuged at 20 000 g for 30 min. After that the supernatants were collected and dried in a rotational vacuum-concentrator. Dry samples were suspended in 30 μL of ACN:DMSO solution (1:1) and centrifuged at 10 000 g. The supernatants were used for HPLC analysis using a gradient of 30%-90% ACN/30min and a fluorescence detector.

3.2.8. Cell viability

To determine the viability of the cells, 15 μL of the cell suspension was taken and mixed with 0.4% trypan blue solution [53]. 10 μL of the obtained solution was added to both chambers of the counting slide and the viability was measured with the cell counting instrument three times for both of the chambers.

3.2.9. Microscopy analysis

For live cell imaging 20 000 cells were seeded on an 8-well microscopy chamber and grown as described above. After 1-2 days of maintenance, the medium was removed and the cells were incubated with the solutions of ARC-compounds (10 μM and 1 μM, total 200 μL) in serum- and antibiotics-free medium containing 1% DMSO and 0.1% Pluronic F-127 for 1 or 2 hours. After the incubation, the solutions were removed and the cells were washed 2 times with PBS buffer and once with indicator-free RPMI buffer (prolonged wash). During the microscopy analysis, cells were kept in 200 μL of HBSS buffer at room temperature. Oligochrome was used as the light source [150 W Xenon high stability lamp, excitation filter 475 (35) nm, emission filter 525 (45) nm]. The experiments were performed at 50 ms exposure time. 20% and 50% of the maximal power of the lamp was used observing compounds ARC-1837 and ARC-1836, respectively. 20x oil objective was used for imaging. The intensities of the images were auto-scaled. Obtained images were analysed and modified (colour adjustment with a 40% increase in intensity and contrast) with ImageJ.

4. Results and discussion

During the previous studies, a highly affine compound ARC-1504 that contains five aspartate residues has been developed as selective probe towards CK2 (Appendix 22) [33]. Unfortunately, unlike oligoarginine-containing ARC-s, ARC-1504 is strongly negatively charged at physiological pH and does not have the intrinsic property to cross the plasma membrane. A common approach for the introduction of negatively charged molecules inside the cells is the esterification of carboxylic groups with AM esters [36-41]. The purpose of this thesis was to apply this approach on an inhibitor for CK2 containing an oligoaspartate.

The peptide part of ARC-1504 had not been optimized previously and therefore the first step was to examine how the number of aspartates influences the affinity of a compound and whether it would be possible to decrease this number in order to reduce the structural complexity. As ARC-1504 contains mainly L-amino acids, it was also necessary to assess how chirality affects binding.

A series of conjugates containing 1-7 D-Asp residues was synthesized according to the published procedures by Fmoc peptide synthesis methods on Wang resin (Appendix 1) [42, 43]. All the compounds were purified with HPLC and analysed with ESI-MS or ICR-HRMS.

Compounds containing TBBi can be easily identified, as natural bromine consists of two stabile isotopes (78.918338 50.69%; 80.916291 49.31%) [54]. Therefore, compounds containing four bromine atoms have a characteristic MS spectrum (Figure 17).

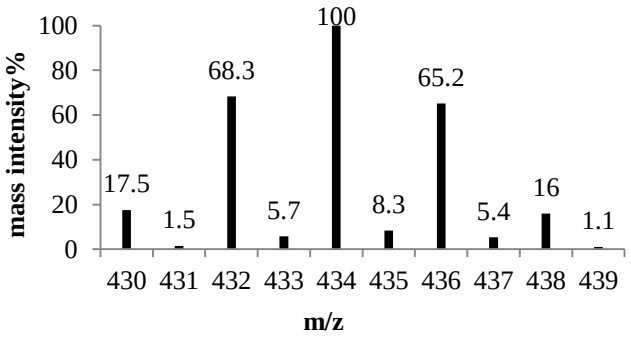

Figure 17. Calculated mass-spectra of protonated TBBi [55].

Purification of compounds containing 4 to 7 aspartate residues (ARC-1804, ARC-1805, ARC-1806 and ARC-1807) resulted in two isomers (marked as I and II), which could be separately collected. The two isomers of ARC-1807 were inseparable and were therefore collected as a mixture. Most probably, the two isomers were α and β peptides due to aspartimide formation in the sequence Asp(OR)-Gly, because this sequence is particularly

prone to the formation of aspartimide [44]. As the synthesis of all the conjugates was carried out in a single vessel by taking an aliquot after every amino acid attachment, the aspartimide formation during the fourth amino acid attachment was 'carried over' to all the consecutive synthesized compounds resulting in formation of two isomers for every compound. Because it is very difficult to determine the structures of the two isomers, the syntheses of compounds containing 4, 5 and 6 aspartates were repeated. This time during every N-terminal deprotection 0.1 M HOBt solution was added to the reaction medium, because this approach is reported to depress the formation of aspartimide; also a resin without previously attached Gly was used [44]. All the compounds were purified with HPLC and analysed with ESI-MS or ICR-HRMS. The chromatograms revealed only one peak with the correct m/z for every synthesis revealing no aspartimide formation had occurred.

The affinities of synthesized inhibitors were measured with fluorescence anisotropy assay. The concentration of the active kinase was determined with a fluorescence anisotropy-based binding assay before every displacement assay. The content of active CK2α$^{1\text{-}335}$ was usually around 20-30% (Figure 18A). In this study, a CK2α$^{1\text{-}335}$ C-terminal deletion mutant comprising amino acids 1-335 was used, because it is more stable as compared to full length human CK2α$^{(1\text{-}391)}$ [56]. When excited with polarized light, kinase-bound portion of ARC-1504 (K_D = 0.4 nM, labelled with fluorescence dye PromoFluor 647, ex/em maximum: 654/672 nm) emits polarized light after excitation [33]. When the fluorescent probe in an unbound state is excited with the polarized light, it emits depolarized light.

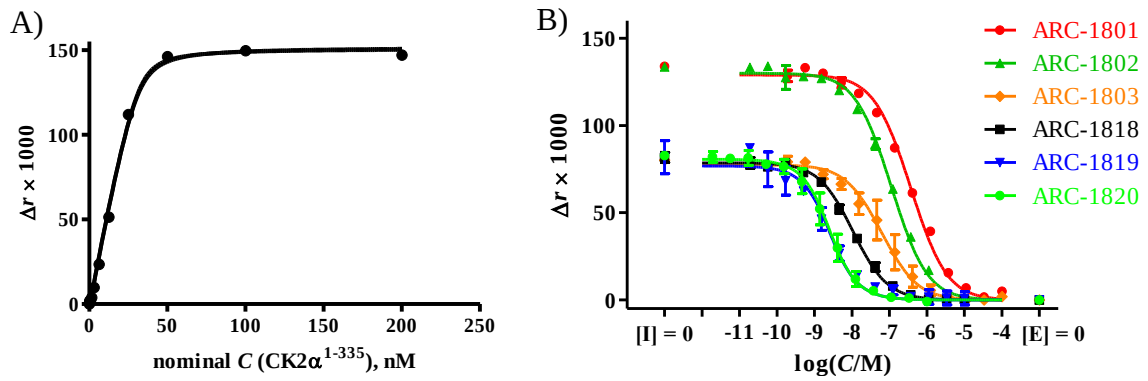

Figure 18. A) Titration of 10 nM ARC-1504 with CK2α$^{1\text{-}335}$ **B)** Displacement curves of non-labelled compounds using ARC-1504 (2 nM with ARC-1801, ARC-1802; 3 nM with the rest) as competitive probe and CK2α$^{1\text{-}335}$ (3 nM with ARC-1801, ARC-1802; 2 nM with the rest).

The affinities of compounds were measured with the displacement assay based on fluorescence anisotropy measurements (Figure 18B, Appendix 23, Table 1). ARC-1504 was used for the affinity measurements of compounds containing 1-6 aspartate residues. As

determination of the affinities of unlabeled compounds is limited by the K_d value of the fluorescent ligand, more affine fluorescent probe ARC-1513o (K_D = 0.01 nM) was used for assaying compounds containing 6-7 aspartate residues (Appendix 22) [57, 58].

Table 1. Affinities of different ARC-type inhibitors determined by the displacement assay.

Number of aspartates	Compounds containing D-Aspartates		Compounds containing L-Aspartates	
	Compound code	K_d (SD), nM	Compound code	K_d (SD), nM
1	ARC-1801	45.2 (3.1)	ARC-1506	43.4 (6.9)
2	ARC-1802	18.5 (7.5)	ARC-1507	26.8 (8.2)
3	ARC-1803	4.03 (0.18)	ARC-1508	4.64 (3.15)
4	ARC-1804 I	2.20 (0.51)		
	ARC-1804 II	1.43 (0.37)		
	ARC-1818	1.56 (0.60)	ARC-1518	2.21 (0.20)
5	ARC-1805 I	0.86 (0.36)		
	ARC-1805 II	0.63 (0.23)		
	ARC-1819	0.80 (0.36)	ARC-1519	1.72 (1.09)
6	ARC-1806 I	0.52 (0.24)		
	ARC-1806 II	0.39 (0.23)		
	ARC-1820	0.52 (0.38)	ARC-1509	0.55 (0.40)
7	ARC-1807 I-II	0.25 (0.12)	n.d.	

The measured affinities of the isomers (I and II) did not differ from each other significantly, indicating that the position of the carboxylate can be altered without having an effect on the affinity of the compound (Table 1, Figure 19).

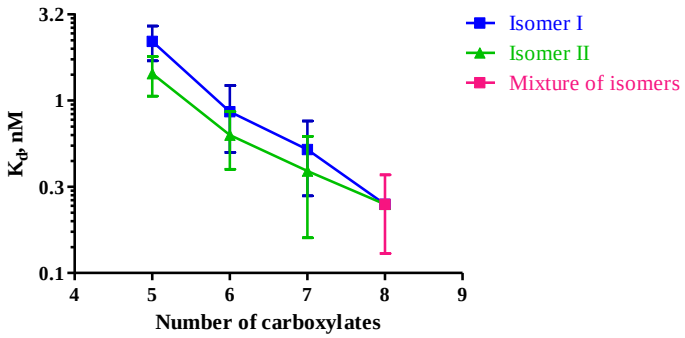

Figure 19. Comparison of the affinities of collected isomers.

According to these results, every additional aspartate residue increased the affinity about 2-3 times (Table 1). A plateau of saturation of affinity was not achieved within this series of compounds and it could be hypothesized that adding subsequent residues would increase the affinity even more. It was also clear that the affinity of a compound could be easily regulated by varying a number of aspartates. For example, attachment of three carboxylic groups to TBBi *via* an adequate linker yields in a 100-fold increase in affinity. The comparison of the compounds containing either D- or L-aspartate residues revealed that the affinities of the conjugates were statistically indistinguishable. These results in combination with the

previously reported crystallographic evidence imply that no fixed interactions are formed between the negative charges of the conjugate and the kinase [33].

Previously, it has been demonstrated that the transformation of carboxylic acids to AM esters in peptides is complicated as the esters are not stable and form aspartimides very easily [59]. There are a few examples, where a cyclic peptide has been esterified, but with highly optimized reaction conditions [37]. As the present work indicated that chirality of inhibitor does not affect affinity in case of CK2 and the peptide fragment can be flexible, it was decided to synthesize compounds incorporating achiral isomers of peptides called peptoids, which are incapable of forming aspartimides.

Eight peptoids containing different number of Nasp groups were synthesized (Figure 20, Appendix 1). *N*-4-aminobutylglycine (Nlys) was added to C-terminals of peptoids to enable the subsequent dye attachment. Previously it has been shown that additional negative charge in the C-terminus of the peptide part has positive effect on the affinity of the compounds [59]. For peptoid synthesis, 2-chlorotrityl chloride resin was used, which enables to synthesize peptoids containing a free C-terminal carboxylate [52]. *Tert*-butyl ester was used as the protection group of the side chains. The progression of the synthesis was monitored with PNBP and chloranil tests [60, 61]. During the synthesis of ARC-1839, the second *N*-carboxymethylglycine (Nasp) was replaced with *N*-methylglycine (Nala) to assess the influence of the second Nasp on the affinity. Nala was added in the form of Fmoc-sarcosine. Finally, TBBi-oca was attached to the peptoid; the product was cleaved from the resin and purified with HPLC. Every additional carboxylate residue increased hydrophilicity of the compound and therefore decreased the retention time in the HPLC analysis. ESI-MS and ICR-HRMS analyses determined a good agreement between theoretical and measured mass spectra.

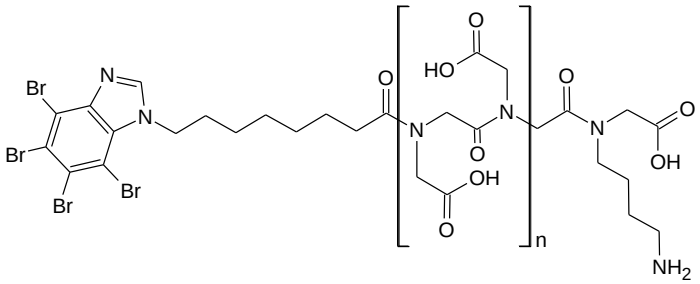

Figure 20. General structure of synthesized peptoids. n = 2…6.

The syntheses of peptides and peptoids are similar in a way that one monomer attachment needs two steps to be completed. An attachment of one amino acid to a peptide chain takes about 2 hours. One monomer attachment in peptoid synthesis takes about 4 hours. When

comparing the time-scale of peptide and peptoid synthesis, the latter one is more time-consuming.

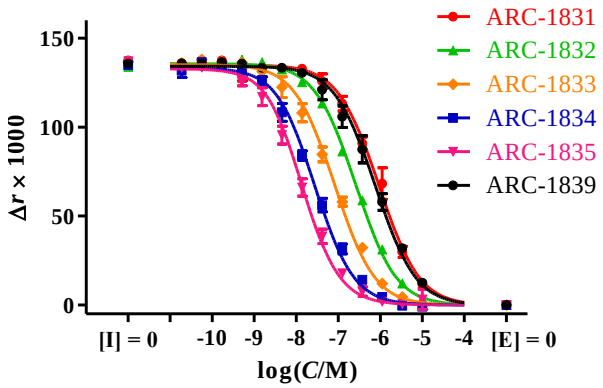

Figure 21. Displacement curves of non-labelled compounds using ARC-1504 (2 nM) as competitive probe and CK2$\alpha^{1\text{-}335}$ (3 nM).

The affinities of peptoids were measured with the displacement assay using ARC-1504 as the fluorescence ligand (Figure 21, Table 2).

Table 2. Structures, codes and affinities of synthesized peptoids. n.d. – not determined.

Inhibitor structure	Compound code	K_d (SD), nM
TBBi-oca-(Nasp)$_2$-Nlys-OH	ARC-1831	131 (52)
TBBi-oca-(Nasp)$_3$-Nlys-OH	ARC-1832	33.3 (2.2)
TBBi-oca-(Nasp)$_4$-Nlys-OH	ARC-1833	10.2 (2.2)
TBBi-oca-(Nasp)$_5$-Nlys-OH	ARC-1834	3.34 (0.65)
TBBi-oca-(Nasp)$_6$-Nlys-OH	ARC-1835	2.18 (1.37)
TBBi-oca-(Nasp)$_3$-(Nlys-BODIPY FL)-OH	ARC-1836	21.5 (2.0)
TBBi-oca-(Nasp-AM)$_3$-(Nlys-BODIPY FL)-AM	ARC-1837	n.d.
TBBi-oca-Nasp-Nala-Nasp-Nlys-OH	ARC-1839	95 (25)

As expected, the affinities increased with the increasing number of Nasp. Yet the measured K_d values were about five times higher than dissociation constants of peptides containing the same number of carboxylates in side chains (Figure 22). This could be caused by positively charged ammonium group in Nlys subunit, which might affect binding negatively as has been reported previously [34]. The K_d value of ARC-1839 (containing 2 Nasp, 1 Nala residues and the C-terminal carboxylate) revealed that the second Nasp influences the affinity notably as the K_d value increased about three times when this Nasp was replaced with Nala. These results provide further supporting info that the peptide binding cleft of protein kinase CK2 is not very sensitive to the exact positions of negative charges in the structure of inhibitors, but rather to the overall charge.

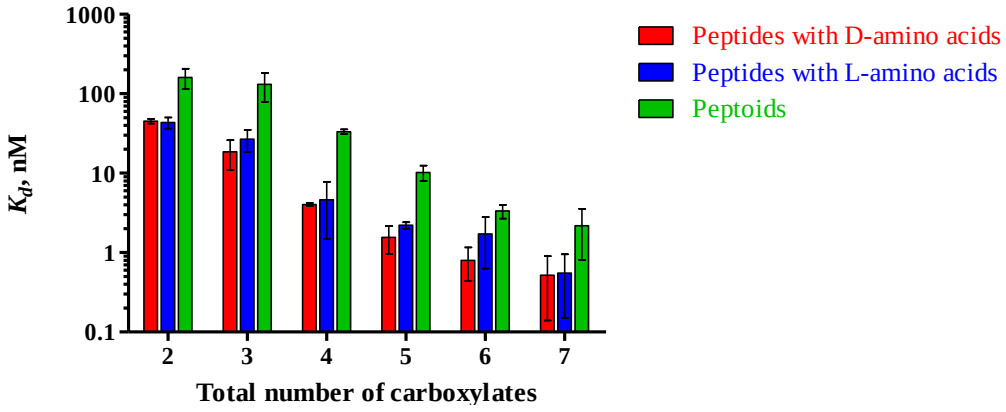

Figure 22. Affinity comparison between synthesized peptides and peptoids.

Compounds containing several carboxylates cannot penetrate a cell membrane because of the large overall negative charge. For the cell experiments the carboxyl groups were masked with AM esters. As AM esters are not very stable, it was reasonable to reduce the number of esters to minimum. Yet, the abundance of carboxylates was essential as every additional carboxylate increased the affinity of a compound. In this study a peptoid with three carboxyl side groups was chosen for the pilot test. For the esterification, the compound ARC-1836 was reacted with bromomethyl acetate in DMF in the presence of base overnight. The chromatographic analysis of the synthesis revealed five separate peaks with MS spectra that corresponded to compounds with different number AM ester groups, which means that the reaction did not proceed to the end at conditions described above and needs to be optimized. The product (ARC-1837) peak was collected and analysed with HRMS that confirmed the agreement of the theoretical and measured MS spectra. The K_d value of ARC-1837 decreased compared to the affinity of unesterified compound ARC-1836, which supports the idea that elimination of the positive charge near the C-terminus increases the affinity of the compound.

In order to make the compound visible inside a cell, a fluorescence dye BODIPY FL C_5 was attached to the inhibitor. BODIPY FL was chosen because of its excellent optical properties, lack of overall charge and small size. The synthesis took place in DMF with triethylamine for 6 hours. HPLC analysis revealed one major peak and HRMS analysis confirmed a good agreement between theoretical and measured mass spectra.

As AM esters are known to be prone to hydrolysis, the hydrolytic stability of ARC-1837 was examined with HPLC (Figure 23) [40]. About 6% of ARC-1837 was decomposed when stored in DMSO solution at 2.1 mM concentration for one month at -20 °C as revealed by HPLC analysis. The chromatogram after 1.5 hour incubation in assay buffer revealed that the initial esterified compound ARC-1837 had hydrolysed further. The peak corresponding to

ARC-1837 covered about 82% of the total peak area after 1.5 hours and about 80% after three hours.

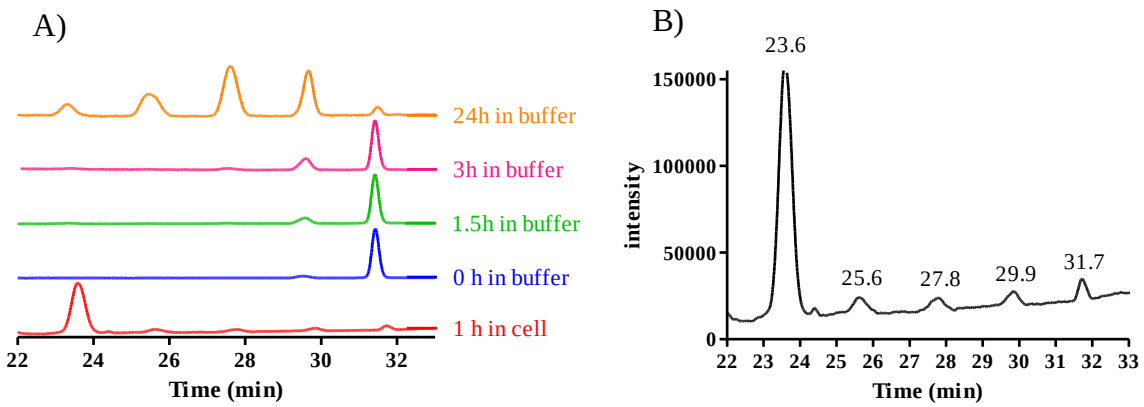

Figure 23. Hydrolysis of ARC-1837 at 37 °C in buffer (pH = 7.5, **A**) and in cell (1 h, **A** and **B**). Chromatograms are normalized according to the peak with the highest intensity.

After incubation in buffer for 24 hours, the fully esterified compound was almost completely decomposed as the peak corresponding to non-decomposed ARC-1837 covered only about 6% of the total peak area, although there were present several intermediate compounds in considerable amounts. To verify that those five peaks correspond to compounds differing in the number of ester groups, as it was observed in the purification of the reaction mixture of the esterification, attempts to measure ESI-MS spectra were made. Unfortunately the signals of the compounds were not high enough for acceptable signal-to-noise ratio in ESI-MS measurement, possibly due to the presence of detergents. To determine the m/z of the decomposition products, the hydrolysis was repeated using a 1 mM solution of ARC-1837 in a 50:50 mixture of DMSO and buffer (without detergent) as the solvent for proper dissolution of ARC-1837 and incubating at 70 °C for 4 hours. Before the HPLC-MS analysis, some non-decomposed ARC-1837 was added to the hydrolysis solution to assure the presence of all the compounds differing in number of ester groups. The retention times of the products from the latter hydrolysis match to the retention times of the products from the first hydrolysis experiment. An external calibration was used (chromatogram and ESI-MS spectra prior to the calibration are present in Appendix 21). The mass spectra of the peaks that appear as the result of decomposition indeed match to the mass-spectra of compounds lacking one, two, three or four AM ester groups (Table 3).

Table 3. Mass-spectra of decomposition products compared with theoretical spectra.

Peak	**Retention time (min)**	**ESI-MS $[M+H^+]^+$ (achieved with external calibration)**	**Calculated base peak $[M+H^+]^+$**
1	23.2	1352	ARC-1836: 1352.1137
2	25.5	1424	ARC-1837 – 3 AM ester: 1424.5478
3	27.6	1496	ARC-1837 – 2 AM ester: 1496.6105
4	29.6	1569	ARC-1837 – 1 AM ester: 1568.6733
5	31.5	1640	ARC-1837: 1640.1982

Next, compound ARC-1837 was applied in cell experiments to test the cellular uptake of the compound. Most of the earlier cellular experiments with ARC-compounds and compounds containing AM-esters have used up to a 10 μM solution and an incubation time of 1 hour, therefore similar conditions were applied [29, 62]. The experiments were carried out at 1 and 10 μM concentrations of fluorescent compounds using HeLa cells and with 1 and 2 hour incubation periods. As a reference, cells were also incubated with unesterified compound ARC-1836. The localization of the fluorescent compound inside the cells can be seen from the obtained microscopy images (Appendix 24). The compound ARC-1837 is distributed in the cytoplasm in every cell, while the cell nuclei are less stained. The latter observation is dramatically different from the previous studies with arginine-rich ARCs which stained intensely speckles in the cell nuclei (probably due to interaction with negatively charged DNA or RNA present in the nucleus). Therefore, nuclear exclusion serves as an indirect evidence for the fact that carboxylate-rich ARCs possess reduced non-specific binding to nucleic acids. However, it should be noted that for CK2 itself, both cytoplasmic and nuclear localization has been reported [21]. Still, it is possible that inhibition of CK2 might have promoted its transport out of the nucleus, which remains to be established in future experiments.

ARC-1837 also stained more intensely some bright spots near cell nuclei, which could represent microtubule-rich area near the centrosome (in interphase, centrosome(s) are attached to the nuclear membrane); importantly, centrosomal enrichment of CK2 has also been previously reported [62]. Further studies (e.g., cross-staining of well-established centrosomal components) will be required to confirm this notion. Interestingly, in case of increased cell confluence, intense staining of the cell plasma membrane by ARC-1837 was also evident; however, this might have been caused by non-specific binding of relatively hydrophobic BODIPY moiety to the membrane regions with increased thickness. A compound with a different fluorescent label could be synthesized to test this hypothesis.

Compound ARC-1836 (without AM esters) has poorly entered the cells and does not have a diffuse distribution. In contrast to ARC-1837, the non-esterified ARC-1836 possessed strongly endosomal staining pattern. During the observation of the cell membrane-permeation of ARC-1836, the required intensity of the light source for a decent signal to noise ratio was 2.5 times higher than for ARC-1837 due to weaker fluorescence signal of the former compound. Overall, it was confirmed that introduction of AM esters strongly facilitates the uptake of carboxylate-rich compounds in the cells, and results in profoundly changed staining profile (i.e., as compared to the non-esterified compound).

Determination of the viability of the cells after treatment with an inhibitor is essential, if the probe is used as a tool for studying cellular processes. For cell viability experiments HeLa cells were incubated with 10 μM ARC-1837 for 1 hour and the viability was measured with a cell counter using instructions provided from the manufacturer [53]. For comparison cells were also incubated with a solution that did not include ARC-1837. The proportion of live cells over total cells was 88% (SD 3%) when incubated with medium containing ARC-1837 and 82% (SD 8%) when incubated without ARC-1837. These results indicate that during the incubation period of 1 hour the cell viability is not affected by the presence of ARC-1837.

For the effective binding between the inhibitor and CK2, the ester groups of ARC-1837 need to be hydrolysed. The chromatographic analysis of intracellular stability of ARC-1837 revealed a dominating peak, which corresponded to the completely hydrolysed compound ARC-1836 (Figure 23). In addition, there was a smaller peak with R_f value of 31.7 min, which corresponded to the R_f value of the initial compound ARC-1837. Between these peaks, there were three small peaks with R_f values equal to the R_f values of previously determined hydrolysis products, which indicated with high probability that most of the AM ester groups of ARC-1837 had been hydrolysed. As ARC-1837 was used in cell experiments within maximally 2.5 hours, the decomposition of ester groups in such short time-scale could not be attributed to hydrolysis initiated by water only, but also by intracellular esterases. Yet, hydrolysis of all ester groups was incomplete, which has also been reported previously for AM esters of calcium sensors [64].

Summary

The purpose of this study was to develop a cell membrane permeable inhibitor for CK2. To accomplish this goal, it was initially necessary to establish how the affinities of ARC-type compounds depend on the chirality and on the number of amino acids. For that reason, 7 inhibitors containing different number of D-Aspartate residues were synthesized. Their affinities were measured and compared to affinities of inhibitors containing the same number of L-Aspartate residues synthesized by Jürgen Vahter. The binding experiments revealed that the affinity did not depend considerably on chirality and that the K_d values of the synthesized inhibitors decreased about three times with every additional aspartate residue.

As an aspartate residue is negatively charged in a physiological environment, compounds containing several aspartates are incapable of permeation the cell membrane. Utilization of prodrug approach with AM esters to mask negatively charged groups is a possible way to overcome the problem. After the compound crosses the plasma membrane, intracellular esterases cleave the esters to release the original compound. As peptides containing AM esters are generally unstable and form aspartimides very easily, peptide isomers called peptoids can be used instead. Five peptoids containing different number of Nasp monomers were synthesized and their affinities were measured in biochemical assay with CK2. A peptoid containing three Nasp monomers with a K_d value of 33.3 nM was chosen for cell experiments. A fluorescent dye was attached to the peptoid and its carboxylates were esterified.

The acquired esterified compound ARC-1837 but also the unesterified compound ARC-1836 were applied to cell experiments. Microscopy analyses verified that ARC-1837 permeated the cell membrane much more easily than ARC-1836. Hydrolysis experiments in buffer were conducted to examine the stability of AM esters in aqueous environment. The compound was quite stable over the time range that was used in cell experiments. The intracellular stability of ARC-1837 was examined and the results showed that after 1 h incubation in cell, the initially esterified compound ARC-1837 had lost most of its ester groups. It can be hence concluded that the AM esters are efficiently cleaved by intracellular esterases.

To sum up, in this work a new cell membrane-permeable esterase-activated inhibitor of CK2 was designed and synthesized. It was demonstrated that the compound possessed low nanomolar affinity in the biochemical studies, permeated the cell membrane and was activated by intracellular esterases.

Proteiinkinaasi CK2 polüanioonsete inhibiitorite derivatiseerimine nende efektiivseks transpordiks rakkudesse

Siiri Saaver

Kokkuvõte

CK2 on kinaas, mis osaleb väga paljudes rakuprotsessides. Tema liigset aktiivsust rakus seostatakse erinevate haigustega, mistõttu on CK2 saanud üheks ravimitööstuse sihtmärgiks. Varasemalt on Asko Uri uurimisrühmas arendatud CK2 jaoks kõrgafiinseid ja selektiivseid inhibiitoreid, kuid need on negatiivselt laetud ja seetõttu rakumembraani edukalt läbida ei suuda. Atsetoksümetüülestritega on võimalik negatiivsed laengud maskeerida rakumembraani läbimise ajaks ning rakus hüdrolüüsitakse ühend esteraaskatalüütiliselt algseks laengutega konjugaadiks.

Käesoleva töö eesmärgiks oli välja arendada ARC-tüüpi rakkusisenev inhibiitor proteiinkinaasi CK2 jaoks. Esmalt uuriti asparagiinhapete arvu ja kiraalsuse mõju inhiibitori afiinsusele. Selle jaoks sünteesiti seitse TBBi-oligoaspartaadi konjugaati, mis sisaldasid 1-7 D-asparagiinhappe jääki. Saadud ainete võimet seonduda proteiinkinaasiga CK2 võrreldi Jürgen Vahteri poolt sünteesitud L-asparagiinhappe jääke sisaldavate ühendite afiinsustega. Selgus, et ühendite dissotsiatsiooni-konstandid ei sõltu märgatavalt neis sisalduvate aminohapete kiraalsusest. See-eest afiinsus kasvas märgatavalt iga lisatud asparagiinhappega.

Kuna atsetoksümetüülestreid sisaldavad peptiidid on väga ebastabiilsed ning moodustavad kergesti aspartimiide, on võimalik kasutada peptoide peptiidide asemel. Sünteesiti viis peptoidi, mis sisaldasid erineva arvu karboksüülrühmi sisaldavaid külgahelaid. Saadud ühendite afiinsused mõõdeti ning edasisteks eksperimentideks valiti konjugaat, mis sisaldas nelja karboksüülrühma. Valitud ühendile kinnitati fluorestsentsvärv ning ühendist valmistati atsetoksümetüülester.

Näidati, et saadud TBBi-peptoidkonjugaat siseneb AM estri vormis efektiivselt rakku ning hüdrolüüsitakse rakusiseselt lähteühendiks.

References

1. Schwartz, P. A.; Murray, B. W. Protein Kinase Biochemistry and Drug Discovery. *Bioorg. Chem.* **2011**, *39*, 192–210.
2. Dhanasekaran, N.; Reddy, E. P. Signaling by Dual Specificity Kinases. *Oncogene* **1998**, *17*, 1447-1455.
3. Shugar, D. The NTP Phosphate Donor in Kinase Reactions: Is ATP a Monopolist? *Acta Biochim. Pol*. **1996**, *43*, 9-23.
4. Becher, I.; Savitski, M. M.; Savitski, M. F.; Hopf, C.; Bantscheff, M.; Drewes, G.; Affinity Profiling of the Cellular Kinome for the Nucleotide Cofactors ATP, ADP and GTP. *ACS Chem. Biol.* **2012**, *8*, 599-607.
5. Manning, G.; Whyte, D. B.; Martinez, R.; Hunter, T.; Sudarsanam, S. The Protein Kinase Complement of the Human Genome. *Science* **2002**, *298*, 1912-1934.
6. Parsons, M.; Worthey, E. A.; Ward, P. N.; Mottram, J. C. Comparative Analysis of the Kinomes of Three Pathogenic Trypanosamtids: *Leishmania major, Trypanasoma brucei* and *Trypanosoma cruzi*. *BMC Genomics* **2005**, *6*, 127.
7. Hanks, S. K.; Hunter, T. The Eukaryotic Protein Kinase Superfamily: Kinase (Catalytic) Domain Structure and Classification. *FASEB J*. **1995**, *9*, 576-596.
8. Cohen, P.; Alessi, D. R. Kinase Drug Discovery – What's Next in the Field? *ACS Chem. Biol.* **2013**, *8*, 96-104.
9. Knight, Z. A.; Shokat, K. M. Features of Selective Kinase Inhibitors. *Chem. Biol.* **2005**, *12*, 621-637.
10. Cozza G.; Bortolato A.; Moro S. How Druggable Is Protein Kinase CK2? *Med. Res. Rev.* **2010**, *30*, 419-462.
11. Lolli, G.; Pinna, L. A.; Battistutta, R. Structural Determinants of Protein Kinase CK2 regulation by Autoinhibitory Polymerization. *ACS Chem. Biol.* **2012**, *7*, 1158-1163.
12. Kramerov, A. A.; Ljubimov, A. V. Focus on Molecules: Protein Kinase CK2. *Exp. Eye. Res.* **2011**, *101*, 111-112.
13. Meggio, F.; Boldyreff, B.; Marin, O.; Pinna, L. A.; Issinger, O.-G. Role of the β Subunit of Casein Kinase-2 on the Stability and Specificity of the Recombinant Reconstituted Holoenzyme. *Eur. J. Biochem.* **1992**, *204*, 293-297.
14. Meggio, F.; Boldyreff, B.; Marin, O.; Marchiori, F.; Perich, J. W.; Issinger, O.-G. Pinna, L. A. The Effect of Polylysine on Casein-Kinase-2 Activity Is Influenced by Both Structure of the Protein/Peptide Substrates and the Subunit Composition of the Enzyme. *Eur. J. Biochem*. **1992**, *205*, 939-945.

15. Niefind, K.; Raaf, J.; Issinger, O.-G. Protein Kinase CK2: From Structures to Insights. *Cell. Mol. Life Sci.* **2009**, *66*, 1800-1816.
16. Salvi, M.; Sarno, S.; Cesaro, L.; Nakamura, H.; Pinna, L. A. Extraordinary Pleiotropy of Protein Kinase CK2 Revealed by Weblogo Phosphoproteome Analysis. *Biochim. Biophys. Acta* **2009**, *1793*, 847-859.
17. Pinna, L. Protein Kinase CK2: a Challenge to Canons. *J. Cell. Sci.*, **2002**, *115*, 3873-3878.
18. Marin, O.; Meggio, F.; Sarno, S.; Cesaro, L.; Pagano, M. A.; Pinna, L. A. Tyrosine *Versus* Serine/Threonine Phosphorylation by Portein Kinase Casein Kinase-2. *J. Biol. Chem.* **1999**, *274*, 29260-29265.
19. Dobrowolska, G.; Lozeman, F. J.; Li, D.; Krebs, E. G. CK2, a Protein Kinase of the Next Millennium. **1999**, *191*, 3-12.
20. Cozza, G.; Pinna, A.L. Moro, S. Kinase CK2 Inhibition: An Update. *Curr. Med. Chem.* **2013**, *20*, 671-693.
21. Faust, M.; Montenarh, M. Subcellular Localization of Protein Kinase CK2. A Key to Its Function? *Cell Tissue Res.* **2000**, *301*, 329-340.
22. Ruzzene, M.; Pinna, L. A. Addiction to Protein Kinase CK2: A Common Denominator of Diverse Cancer Cells? *Biochim. Biophys. Acta* **2010**, *1804*, 499-504.
23. Marschke, R. F.; Borad, M. J.; McFarland, R. W.; Alvarez, R. H.; Lim, J. K.; Padgett, C. S.; Von Hoff, D. D.; O'Brien, S. E.; Northfelt, D. W. *Findings from the Phase I Clinical Trials of CX-4945, an Orally Available Inhibitor of CK2*; http://pressitt.com/public/files/2011/06/02/4906/Cylene_ASCO_2011_CX-945_Phase1.pdf last visited 26.05.2014.
24. Study of CX-4945 in Combination With Gemcitabine and Cisplatin for Frontline Treatment of Cholangiocarcinoma; https://clinicaltrials.gov/ct2/show/NCT02128282?term=CX-4945&rank=1 last updated 29.04.2014
25. Pierre, F.; Chua, P. C.; O'Brien, S.; Siddiqui-Jain, A.; Bourbon, P.; Haddach, M.; Michaux, J.; Nagasawa, J.; Schwaebe, M. K.; Stefan, E.; Vialettes, A.; Whitten, J. P.; Chen, T. K.; Darjania, L.; Stansfield, R.; Anderes, K.; Bliesath, J.; Drygin, D.; Ho, C.; Omori, M.; Proffitt, C.; Streiner, N.; Trent, K.; Rice, W. G.; Ryckman, D. M. Discovery and SAR of 5-(3-Chlorophenylamino)benzo[c][2,6]naphthyridine-8-carboxylic Acid (CX-4945), the First Clinical Stage Inhibitor of Protein Kinase CK2 for the Treatment of Cancer. *J. Med. Chem.* **2011**, *54*, 635-654.
26. Siddiqui-Jain, A.; Drygin, D.; Streiner, N.; Chua, P.; Pierre, F.; O'Brien, S. E.; Bliesath, J.; Omori, M.; Huser, N.; Ho, C.; Proffitt, C.; Schwaebe, M. K.; Ryckman, D. M.; Rice, W. G.;

Anderes, K. CX-4945, an Orally Bioavailable Selective Inhibitor of Protein Kinase CK2, Inhibits Prosurvival and Angiogenic Signaling and Exhibits Antitumor Efficacy. *Cancer Res.* **2010**, *70*, 10288-10298.

27. Andrzejewska, M.; Pagano, M. A.; Meggio, F.; Brunati, A. M.; Kazimierczuk, Z. Polyhalogenobenzimidazoles: Synthesis and Their Inhibitory Activity against Casein Kinases. *Bioorg. Med. Chem*. **2003**, *11*, 3997-4002.
28. Lavogina, D.; Enkvist, E.; Uri, A. Bisubstrate Inhibitors of Protein Kinases: from Principle to Practical Applications. *ChemMedChem* **2010**, *5*, 23–34.
29. Viira, B. Synthesis of Inhibitors for Protein Kinases PKA and PKB. Master's Thesis, University of Tartu, 2012.
30. Uri, A.; Raidaru, G.; Subbi, J.; Padari, K.; Pooga, M. Identification of the Ability of Highly Charged Nanomolar Inhibitors of Protein Kinases to Cross Plasma Membranes and Carry a Protein into Cells. *Bioorg. Med. Chem. Lett*. **2002**, *12*, 2117-2120.
31. Vaasa, A.; Viil, I.; Enkvist, E.; Viht, K.; Raidaru, G.; Lavogina, D.; Uri, A. High Affinity Bisubstrate Probe for Fluorescence Anisotropy Binding/Displacement Assays with Protein Kinases PKA and ROCK. *Anal. Biochem.* **2009**, *385*, 85-93.
32. Enkvist, E.; Vaasa, A.; Kasari, M.; Kriisa, M.; Ivan, T.; Ligi, K.; Raidaru, G.; Uri, A. Protein-Induced Long Lifetime Luminescence of Nonmetal Probes. *ACS Chem. Biol.* **2011**, *6*, 1052-1062.
33. Enkvist, E.; Viht, K.; Bischoff, N.; Vahter, J.; Saaver, S.; Raidaru, G.; Issinger, O.-G.; Niefind, K.; Uri, A. A Subnanomolar Probe for Protein Kinase CK2 Interaction Studies. *Org. Biomol. Chem*. **2012**, *10*, 8645-8653.
34. Ekambaram, R.; Enkvist, E.; Manoharan, G. B.; Ugandi, M.; Kasari, M.; Viht, K.; Knapp, S.; Issinger, O.-G.; Uri, A. Benzoselenadiazole-Based Responsive Long-Lifetime Photoluminescent Probes for Protein Kinases. *Chemm. Commun.* **2014**, *50*, 4096-4098.
35. Schultz, C.; Vajanaphanich, M.; Harootunian, A. T.; Sammak, P. J.; Barrett, K. E.; Tsien, R. Y. Acetoxymethyl Esters of Phosphates, Enhancement of the Permeability and Potency of cAMP. *J. Biol. Chem.* **1993**, *268*, 6316-6322.
36. Grynkiewicz, G.; Poenie, M.; Tsien, R. Y. A New Generation of Ca^{2+} Indicators with Greatly Improved Fluorescence Properties. *J. Biol. Chem.* **1985**, *260*, 3440-3450.
37. Herfindal, L.; Kasprzykowski, F.; Schwede, F.; Lankiewicz, L.; Fladmark, K. E.; Lukomska, J.; Wahlsten, M.; Sivonen, K.; Grzonka, Z.; Jastorff, B.; Doskeland, S. O. Acyloxymethyl Esterification of Nodularin-R and Microcystin-LA Produces Inactive Protoxins that Become Reactivated and Produce Apoptosis inside Intact Cells. *J. Med. Chem.* **2009**, *52*, 5758-5762.

38. Tsien, R. Y. A Non-Disruptive Technique for Loading Calcium Buffers and Indicators into cells. *Nature* **1981**, *290*, 527-528.
39. Patrick, G. L. *An Introduction to Medicinal Chemistry*, 4th ed.; Oxford: Oxford University Press, 2009, p 442.
40. Paredes, R. M.; Etzler, J. C.; Watts, L. T.; Zheng, W.; Lechleiter, J. D. Chemical Calcium Indicators. *Methods* **2008**, *46*, 143-151.
41. Roe, M. W.; Lemasters, J. J.; Herman, B. Assessment of Fura-2 for Measurements of Cytosolic Free Calcium. *Cell Calcium* **1990**, *11*, 63-73.
42. Merrifield, R. B. Solid Phase Peptide Synthesis. I. The Synthesis of a Tetrapeptide. *J. Am. Chem. Soc.* **1963**, *85*, 2149-2154.
43. Amblard, M.; Fehrentz, J.-A.; Martinez, J.; Subra, G. Methods and Protocols of Modern Solid Phase Peptide Synthesis. *Mol. Biotechnol.* **2006**, *33*, 239-254.
44. Benoiton, N. L. *Chemistry of Peptide Synthesis*; CRC Press, USA, 2006, pp 140-143; 172-176.
45. Kaiser, E., Colescot, R. L., Bossinger, C. D.; Cook, P. I. Color Test for Detection of Free Terminal Amino Groups in Solid-Phase Synthesis of Peptides. *Anal. Biochem.* **1970**, *34*, 595–598.
46. Culf, A. S.; Ouellette, R. J. Solid-Phase Synthesis of *N*-Substituted Glycine Oligomers (α-Peptoids) and Derivatives. *Molecules* **2010**, *15*, 5282-5335.
47. Sanborn, T. J.; Wu, C, W.; Zuckermann, R. N.; Barron, A. E. Extreme Stability of Helices Formed by Water-Soluble Poly-N-Substituted Glycines (Polypeptoids) with α-Chiral Side Chains. *Biopolymers* **2002**, *63*, 12-20.
48. Wu, C. W.; Sanborn, T. J.; Huang, K.; Zuckermann, R. N. Barron, A. E. Peptoid Oligomers with α-Chiral, Aromatic Side Chains: Sequence Requirements for the Formation of Stable Peptoid Helices. *J. Am. Chem. Soc.* **2001**, *123*, 6778-6784.
49. Kirshenbaum, K.; Barron, A. E.; Goldsmiths, R. A.; Armand, P.; Bradley, E. K.; Truong, K. T. V.; Dill, K. A.; Cohen, F. E.; Zuckermann, R. N. Sequence-Specific Polypeptoids: A Diverse Family of Heteropolymers with Stable Secondary Structure. *Proc. Natl. Acad. Sci. USA* **1998**, *95*, 4303-4308.
50. Miller, S. M.; Simon, R. J.; Ng, S.; Zuckermann, R. N; Kerr, J. M.; Moos, W. H. Proteolytic Studies of Homologous Peptide and *N*-Substituted Glycine Peptoid Oligomers. *Bioorg. Med. Chem. Lett*. **1994**, *4*, 2657-2662.
51. Patch, J.A.; Kirshenbaum, K.; Seurynck, S.L.; Zuckermann, R.N.; Barron, A.E. Versatile Oligo(*N*-Subsitituted) Glycines: The Many Roles of Peptoids in Drug Discovery. In

Pseudopeptides in Drug Discovery; Nielsen, P.E., Ed.; Wiley-VCH Verlag, GmbH & Co. KgaA: Weinheim, Germany, 2004; pp. 1-31.

52. Anne, C.; Fournié-Zaluski, M.-C.; Roques, B. P.; Cornille, F. Solid Phase Synthesis of Peptoid Derivatives Containing a Free C-terminal Carboxylate. *Tetrahedron Lett.* **1998**, *39*, 8973-8974.
53. TC20TM Automated Cell Counter Instruction Manual. Biorad, 2011.
54. *The 83rd Edition of the CRC Handbook of Chemistry and Physics*; Holden, N. E.; CRC Press, 2002.
55. Isotope Distribution Calculator and Mass Spec Plotter; http://www.sisweb.com/mstools/isotope.htm last visited 26.05.2014
56. Protein kinase CK2 (alpha 1)1-335 subunit, active human recombinant, expressed in E. coli crystallization grade, Certificate of Analysis, Kinasedetect.
57. Huang, X.; Fluorescence Polarization Competition Assay: The Range of Resolvable Inhibitor Potency Is Limited by the Affinity of the Fluorescent Ligand. *J. Biomol. Screen.* **2003**, *8*, 34-38.
58. Vahter, J. Unpublished results.
59. Saarist, S. Rakumembraani Läbivate Proteiinkinaasi CK2 Bisubstraatsete Inhibiitorite Arendamine. Bakalaureusetöö, Tartu Ülikool, 2013.
60. Vojkovsky, T. Detection of Secondary Amines on Solid Phase. *Peptide Res.* **1995**, *8*, 236-237.
61. Galindo, F.; Altava, B.; Burguete, M. I. Gavara, R.; Luis, S. V. A Sensitive Colorimetric Method for the Study of Polystyrene Merrifield Resins and Chloromethylated Macroporous Monolithic Polymers. *J. Comb. Chem.* **2004**, *6*, 859-861.
62. Pluronic® F-127; http://tools.lifetechnologies.com/content/sfs/manuals/mp03000.pdf last updated 09.01.2008.
63. Faust, M.; Günther, J.; Morgenstern, E.; Montenarh, M.; Götz, C. Specific Localization of the Catalytic Subunits of Protein Kinase CK2 at the Centrosomes. *Cell. Mol. Life Sci.* **2002**, *59*, 2155-2164.
64. Oakes, S. G.; Martin, W. J.; Lisek, C. A.; Powis, G. Incomplete Hydrolysis of the Calcium Indicator Precursor Fura-2 Pentaacetoxymethyl Ester (Fura-2 AM) by cells. *Anal. Biochem.* **1988**, *169*, 159-166.

Acknowledgements

This work was supported by grants from the Estonian Research Council (IUT20-17) and the Estonian Science Foundation (8419 and 8055). ICR-MS measurements were supported by the Estonian National Research and development Infrastructure development programme of measure 2.3 'Promotion of development activities and innovation' (Regulation No. 34) funded by the Enterprise Estonia foundation.

I would like to thank Asko Uri for giving me the opportunity to work in the medicinal chemistry research group. I am highly grateful for my supervisor Kaido Viht, whose enormous support, knowledge, patience and advice has helped me throughout my studies. Special thanks go to Darja Lavõgina, who proof-read my thesis and helped me a lot with cell experiments, microscopy imaging and interpreting the cell images.

I would like to thank Gerda Raidaru for the purification of some of the compounds and for teaching me how to operate with HPLC-ESI-MS instrument. I would also like to thank Hedi Sinijärv for patience and willingness to always answer my questions concerning HPLC analysis.

I am extremely grateful to Tõiv Haljasorg, who performed FT-ICR-MS measurements.

Last but not least, I would like to thank everyone else who has been supportive for me.

Appendices

Appendix 1. Structures and codes of synthesized ARC-type inhibitors.

Appendix 2. MS analyses of synthesized ARC-compounds.

Appendix 3. ARC-1801. A) Chromatogram of the purification B) ESI-MS spectrum

Appendix 4. ARC-1802. A) Chromatogram of the purification B) ESI-MS spectrum

Appendix 5. ARC-1803. A) Chromatogram of the purification B) ICR-HRMS on the next page

Appendix 6. ARC-1804 A) Chromatogram of the purification B) ESI-MS spectrum of the I fraction C) ESI-MS spectrum of the II fraction

Appendix 7. ARC-1805. A) Chromatogram of the purification B) ESI-MS spectrum of the I fraction C) ESI-MS spectrum of the II fraction

Appendix 8. ARC-1806. A) Chromatogram of the purification B) ESI-MS spectrum of the I fraction C) ESI-MS spectrum of the II fraction

Appendix 9. ARC-1807. A) Chromatogram of the purification B) ESI-MS spectrum of the I fraction. C) ESI-MS spectrum of the II fraction.

Appendix 10. ARC-1818. A) Chromatogram of the purification B) ICR-HRMS spectrum on the next page

Appendix 11. ARC-1819 A) Chromatogram of the purification B) ESI-MS spectrum

Appendix 12. ARC-1820 A) Chromatogram of the purification B) ESI-MS spectrum

Appendix 13. ARC-1831 A) Chromatogram of the purification B) ICR-HRMS spectrum on the next page

Appendix 14. ARC-1832 A) Chromatogram of the purification B) ESI-MS spectrum

Appendix 15. ARC-1833 A) Chromatogram of the purification B) ESI-MS spectrum

Appendix 16. ARC-1834 A) Chromatogram of the purification B) ESI-MS spectrum

Appendix 17. ARC-1835 A) Chromatogram of the purification B) ESI-MS spectrum

Appendix 18. ARC-1836 A) Chromatogram at 260 nm detector wavelength B) Chromatogram at 505 nm detector wavelength C) HRMS spectra.

Appendix 19. ARC-1837 A) Chromatogram of the purification at 260 nm detector wavelength B) Chromatogram of the purification at 505 nm detector wavelength C) HRMS spectrum

Appendix 20. ARC-1839 A) Chromatogram of the purification at 260 nm detector wavelength B) ICR-HRMS spectrum on the next page

Appendix 21. Chromatogram of the hydrolysis solution and MS spectra of every chromatographic peak (continues on the next page)

Appendix 22. Structures of ARC-1513o (**A**) and ARC-1504 (**B**).

Appendix 23. Measured pIC50 values of inhibitors.

Appendix 24. Uptake of ARC-1836 and ARC-1837 by HeLa with 1 hour (A-D) and 2 hour (E-H) incubation (continues on the next page). A, E – 1 μM ARC-1836; B, F – 1 μM ARC-1837; C,G – 10 μM ARC-1836; D, H – 10 μM ARC-1837. The required intensity of the light source for ARC-1836 was 2.5 times higher than for ARC-1837 due to weaker fluorescence signal. The images are pseudocoloured.

Appendix 1. Structures and codes of synthesized ARC-type inhibitors.

Structure	Code
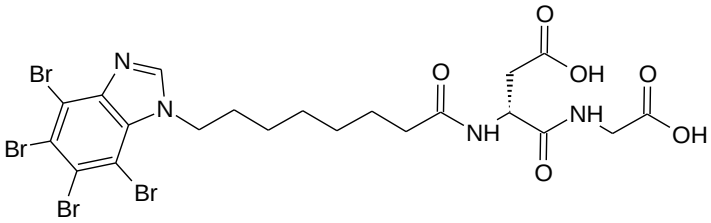	ARC-1801
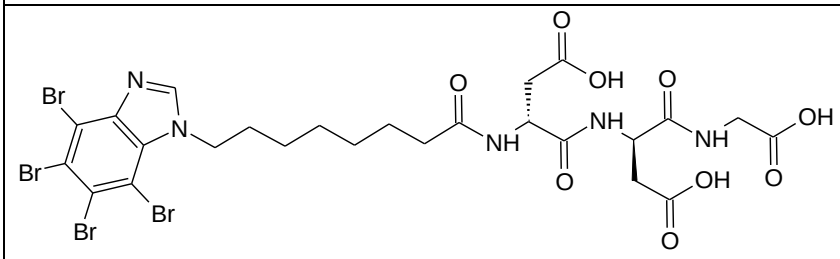	ARC-1802
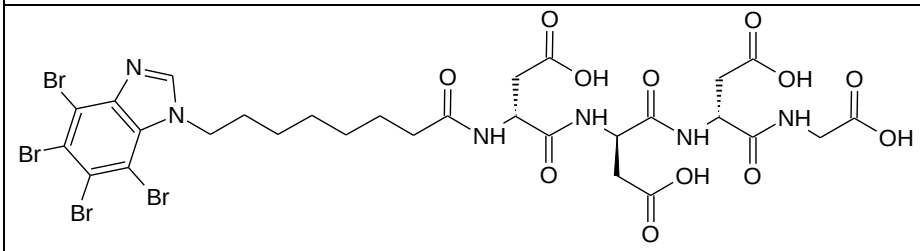	ARC-1803
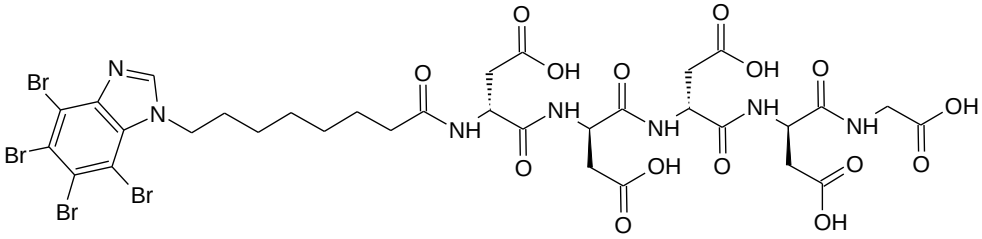	ARC-1804
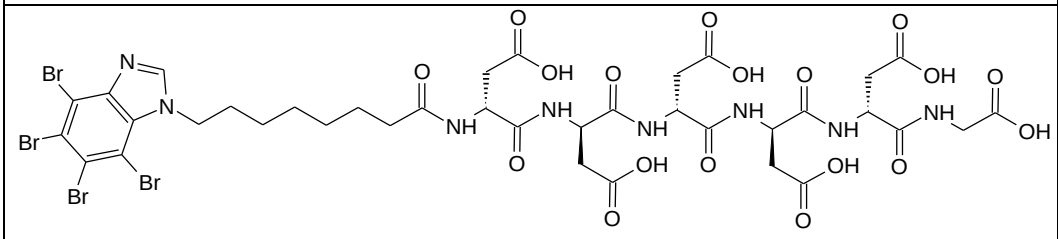	ARC-1805
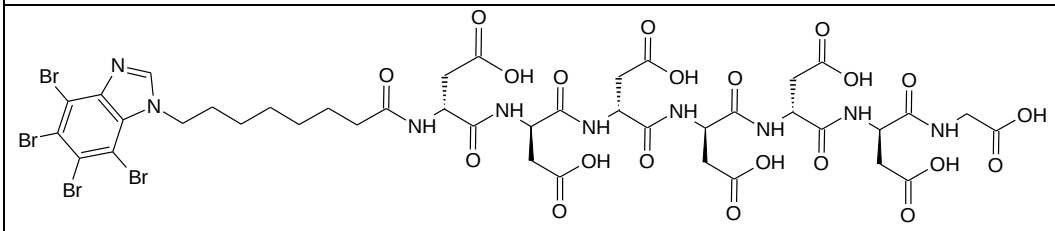	ARC-1806

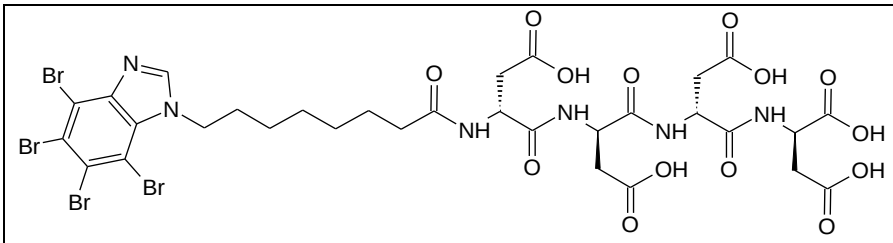	ARC-1818
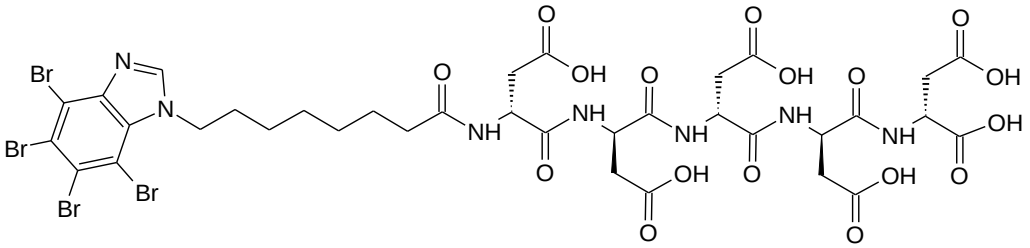	ARC-1819
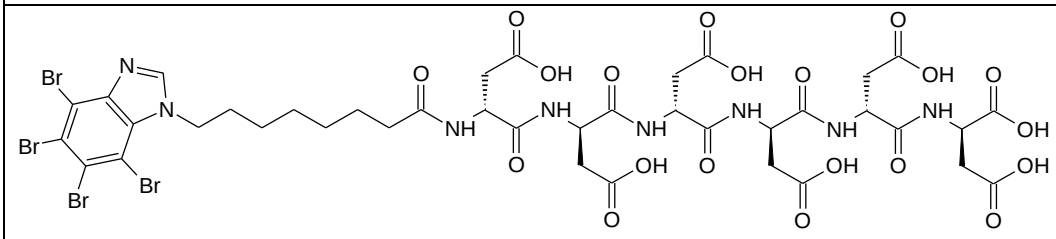	ARC-1820
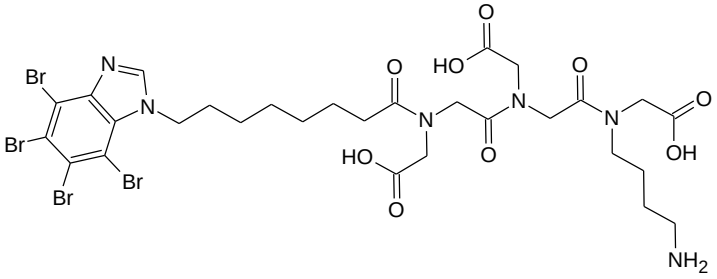	ARC-1831
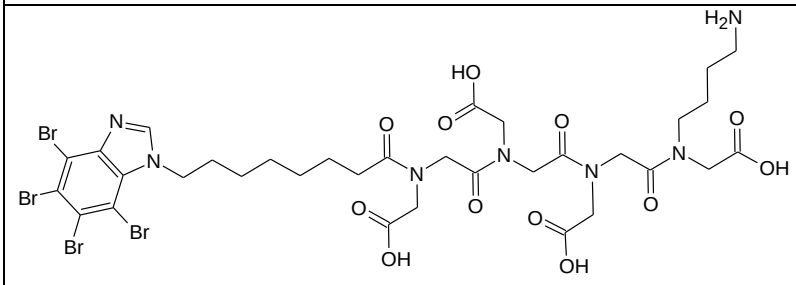	ARC-1832
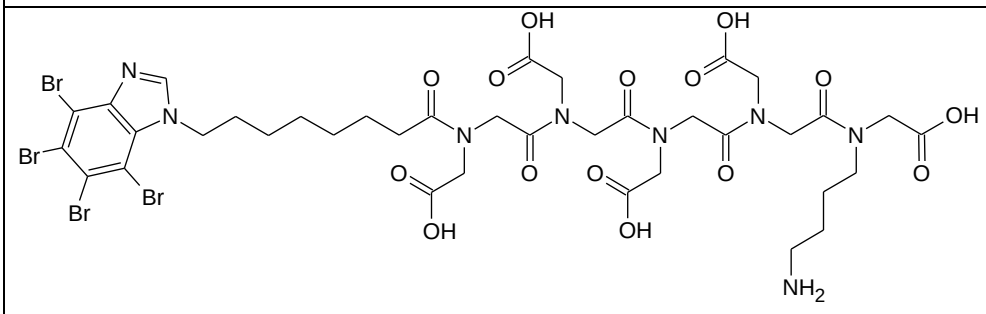	ARC-1833

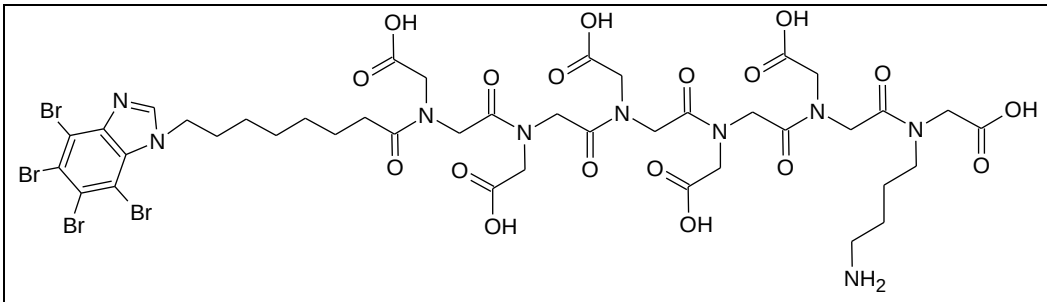	ARC-1834
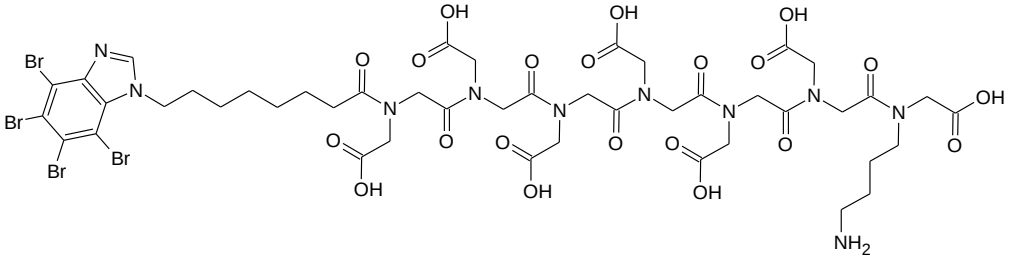	ARC-1835
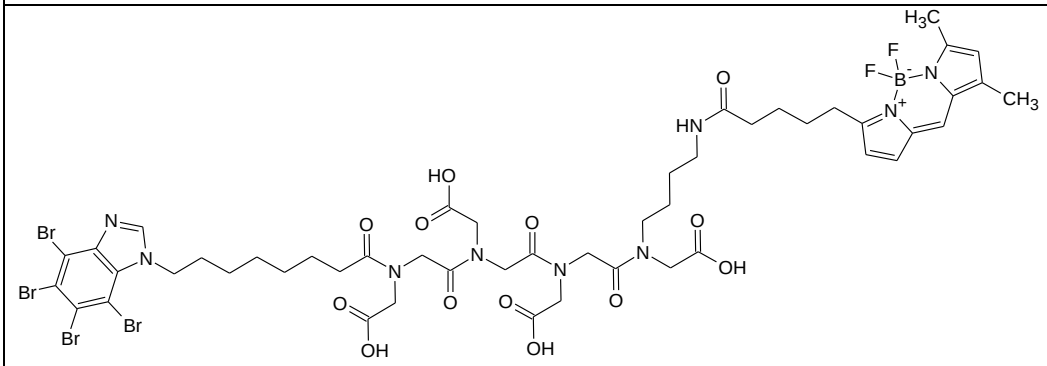	ARC-1836
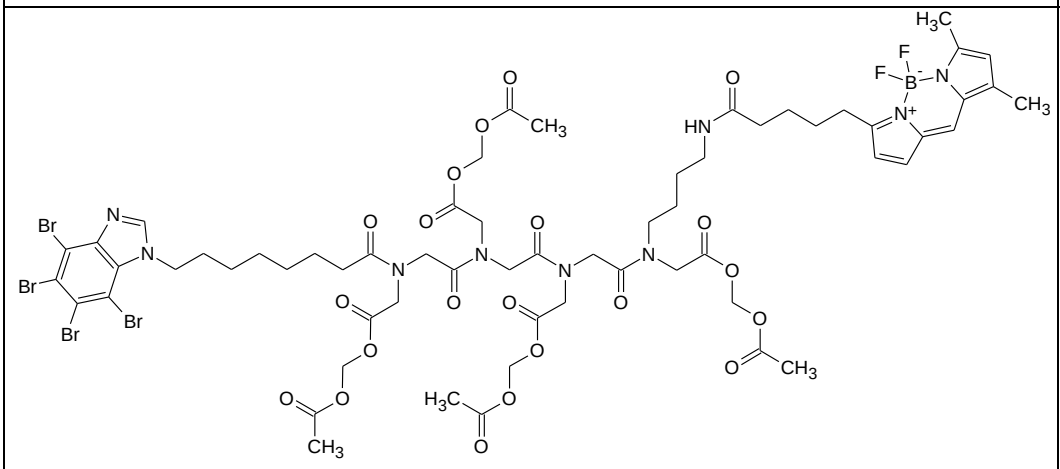	ARC-1837
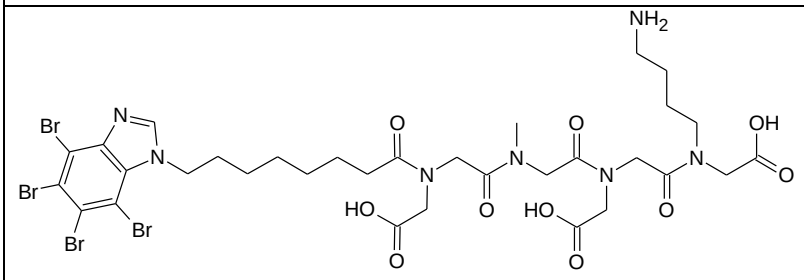	ARC-1839

Appendix 2. MS analyses of synthesized ARC-compounds.

ARC-code	Compound	Calculated base peak $[M+H^+]^+$	R_t (min)	ESI-MS
ARC-1801	TBBi-oca-(D-Asp)-Gly-OH	749	18.2	749
ARC-1802	TBBi-oca-$(D\text{-}Asp)_2$-Gly-OH	864	17.0	864
ARC-1804	TBBi-oca-$(D\text{-}Asp)_4$-Gly-OH	1094	I 15.6 II 15.9	I 1094 II 1094
ARC-1805	TBBi-oca-$(D\text{-}Asp)_5$-Gly-OH	1209	I 14.8 II 15.1	I 1209 II 1209
ARC-1806	TBBi-oca-$(D\text{-}Asp)_6$-Gly-OH	1324	I 14.4 II 14.6	I 1324 II 1324
ARC-1807	TBBi-oca-$(D\text{-}Asp)_7$-Gly-OH	1440	I 14.4 II 14.5	I 1440 II 1440
ARC-1819	TBBi-oca-$(D\text{-}Asp)_5$-OH	1152	15.7	1152
ARC-1820	TBBi-oca-$(D\text{-}Asp)_6$-OH	1267	15.4	1267
ARC-1832	TBBi-oca-$(Nasp)_3$-Nlys-OH	1050	13.3	1050
ARC-1833	TBBi-oca-$(Nasp)_4$-Nlys-OH	1165	13.0	1165
ARC-1834	TBBi-oca-$(Nasp)_5$-Nlys-OH	1281	12.9	1281
ARC-1835	TBBi-oca-$(Nasp)_6$-Nlys-OH	1396	12.8	1396

ARC-code	Compound	Calculated monoisotopic mass $[M+H^+]^+$	R_t (min)	ICR-HRMS	ESI-HRMS
ARC-1803	TBBi-oca-$(D\text{-}Asp)_3$-Gly-OH	974.90464	15.8	974.90422	n.d.
ARC-1818	TBBi-oca-$(D\text{-}Asp)_4$-OH	1032.91012	16.1	1032.91000	n.d.
ARC-1831	TBBi-oca-$(Nasp)_2$-Nlys-OH	930.95120	13.7	930.94977	n.d.
ARC-1836	TBBi-oca-$(Nasp)_3$-(Nlys-BODIPY FL)-OH	1348.1178	22.5	n.d.	1348.1191
ARC-1837	TBBi-oca-$(Nasp\text{-}AM)_3$-(Nlys-BODIPY FL)-AM	1636.2023	24.7	n.d.	1636.2044
ARC-1839	TBBi-oca-Nasp-Nala-Nasp-Nlys-OH	1001.98831	13.3	1001.98805	n.d.

Appendix 3. ARC-1801. A) Chromatogram of the purification B) ESI-MS spectrum.

A)

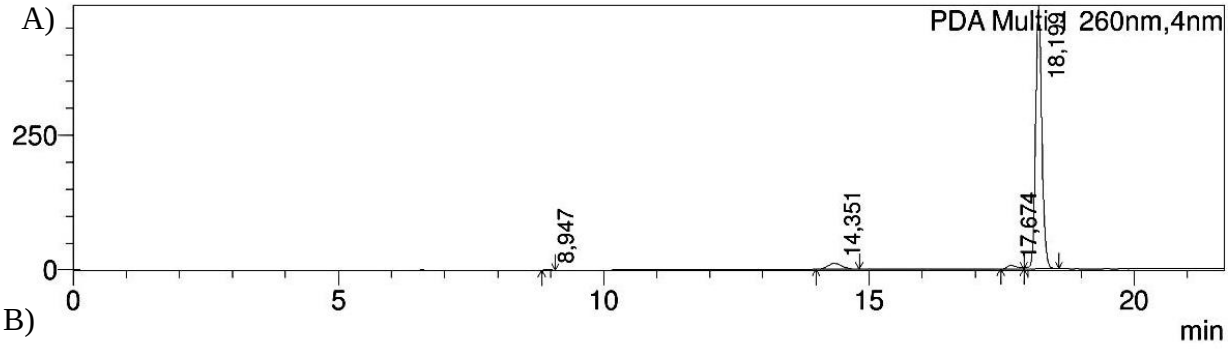

B)

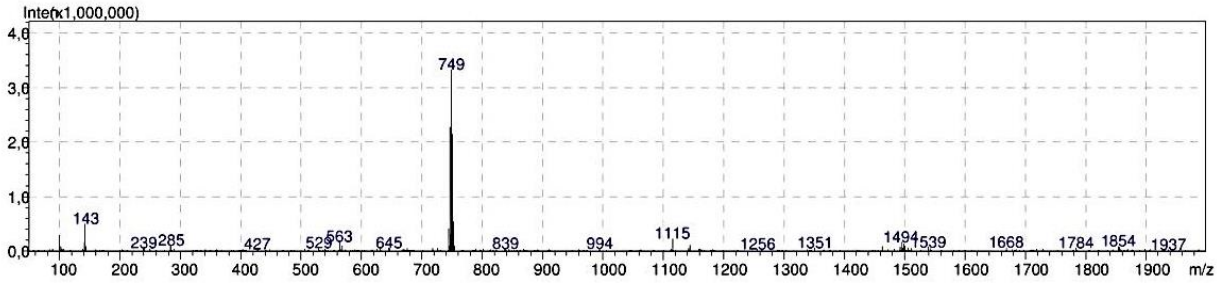

Appendix 4. ARC-1802. A) Chromatogram of the purification B) ESI-MS spectrum.

A)

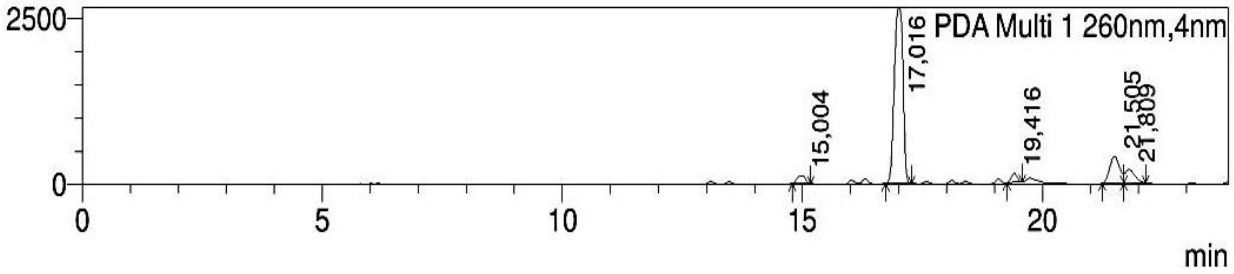

B)

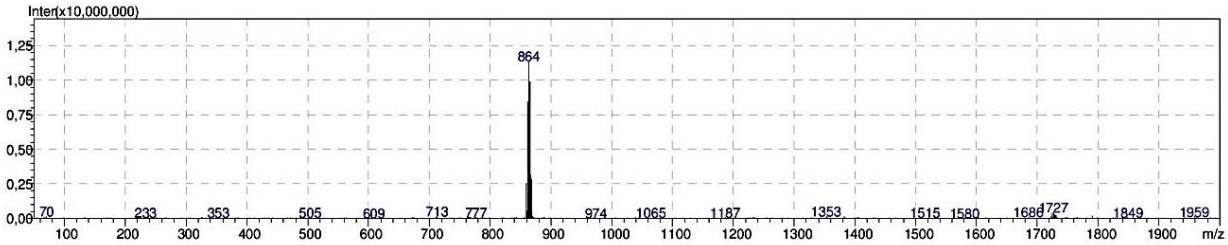

Appendix 5. ARC-1803. A) Chromatogram of the purification B) ICR-HRMS on the next page.

A)

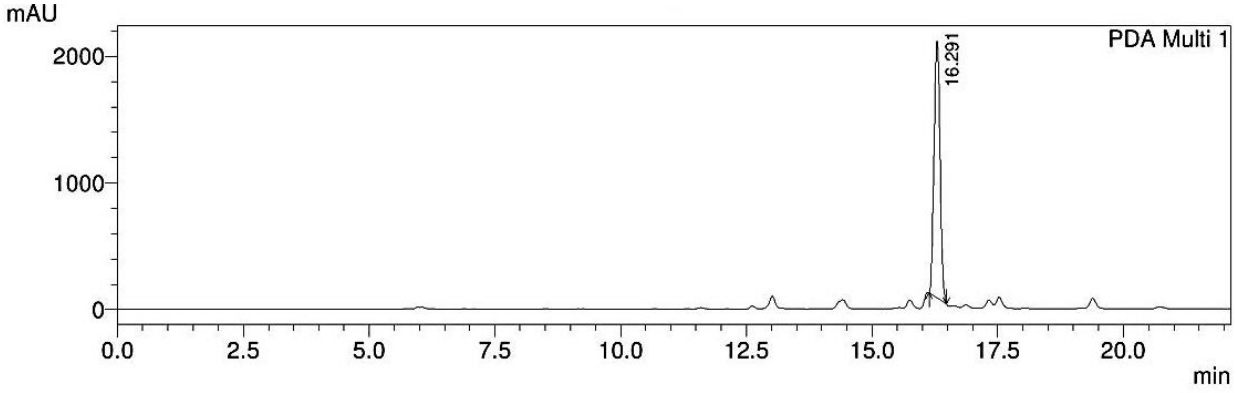

B)

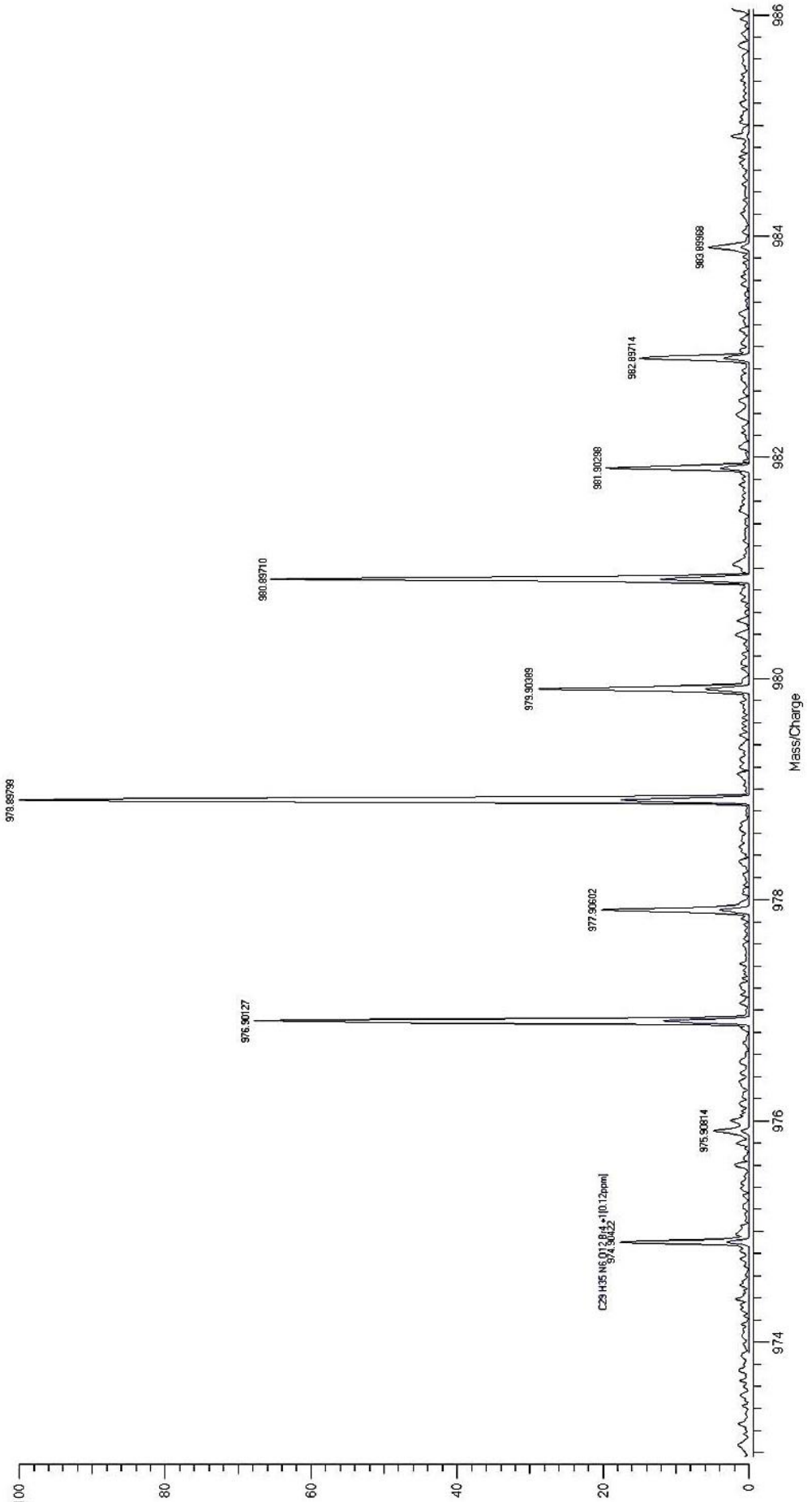
100
80
60
40
20
0
974
976
978
980
982
984
986
Mass/Charge
975.90814
976.90127
977.90602
978.89798
979.90389
980.89710
981.90298
982.89714
983.89968
C29 H35 N6 O12 B I4 +1 [0.12ppm]
974.90422

Appendix 6. ARC-1804 A) Chromatogram of the purification B) ESI-MS spectrum of the I fraction C) ESI-MS spectrum of the II fraction.

A)

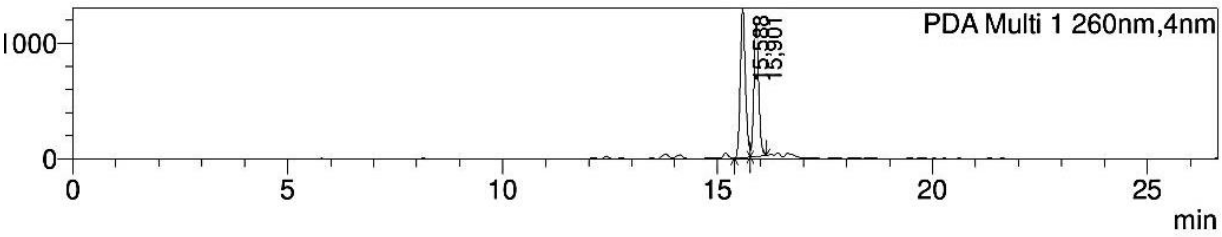

B)

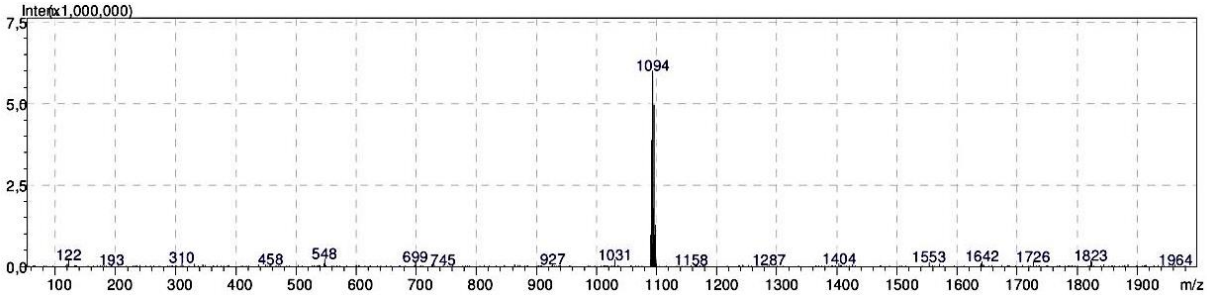

C)

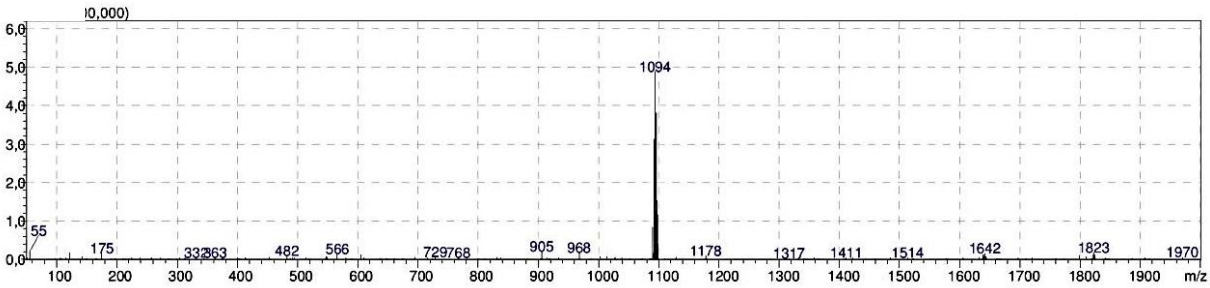

Appendix 7. ARC-1805. A) Chromatogram of the purification B) ESI-MS spectrum of the I fraction C) ESI-MS spectrum of the II fraction.

A)

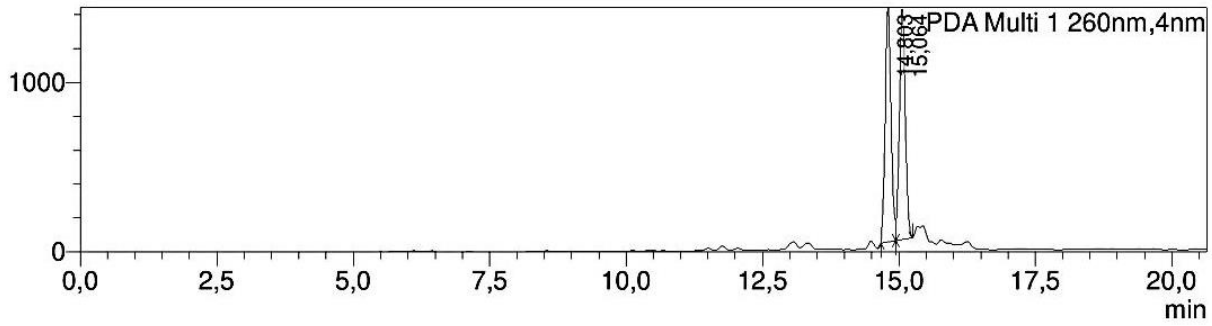

B)

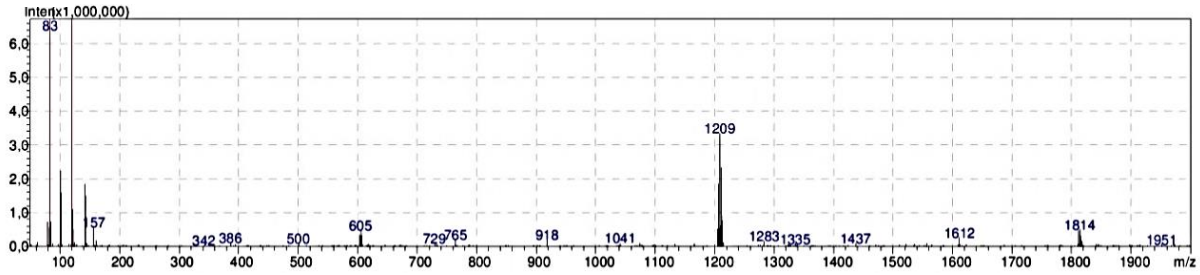

C)

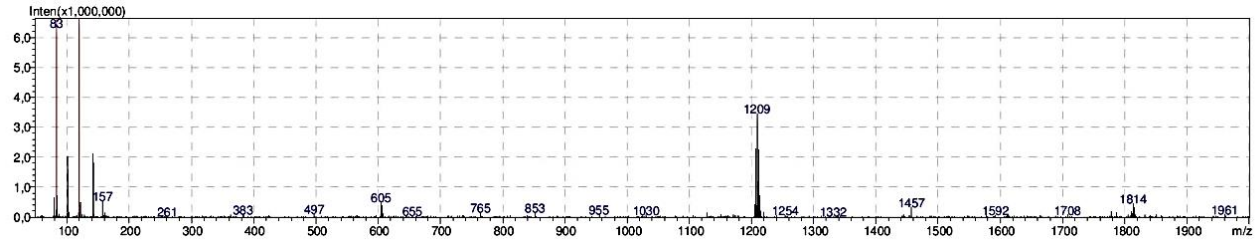

Appendix 8. ARC-1806. A) Chromatogram of the purification B) ESI-MS spectrum of the I fraction C) ESI-MS spectrum of the II fraction.

A)

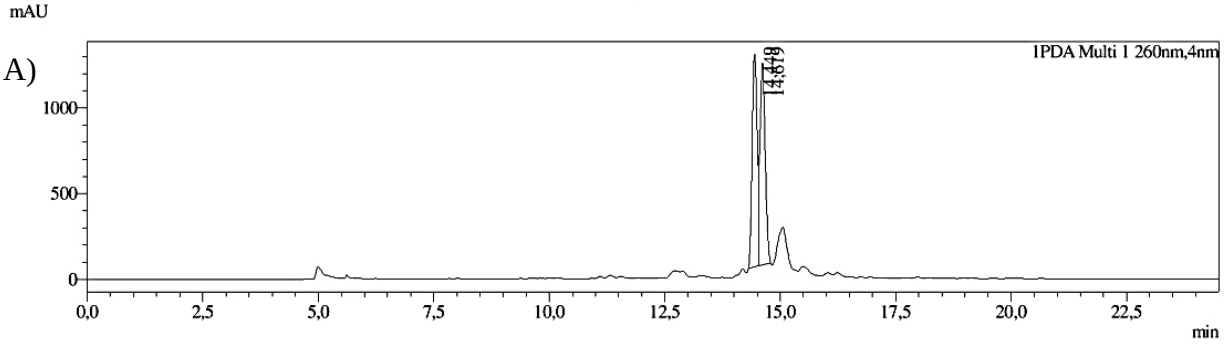

B)

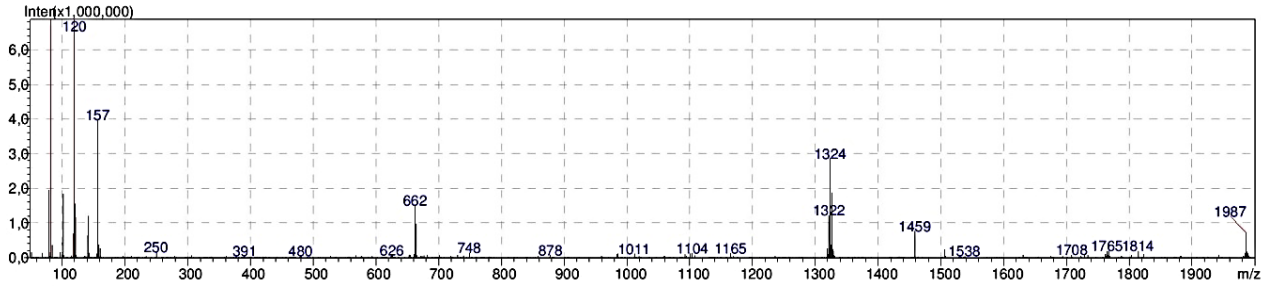

C)

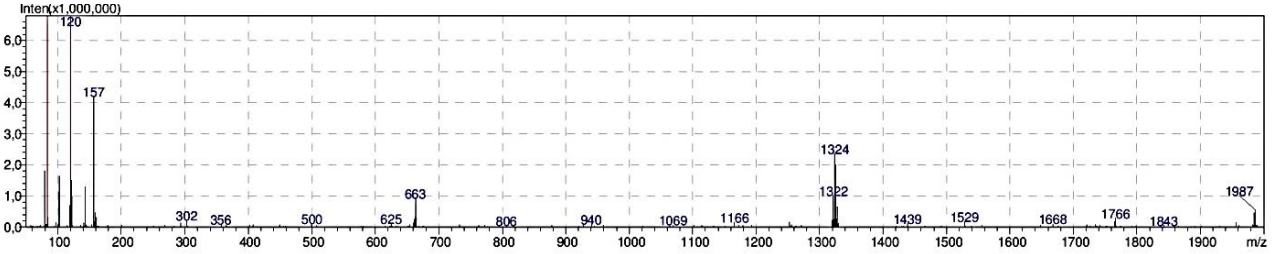

Appendix 9. ARC-1807. A) Chromatogram of the purification B) ESI-MS spectrum of the I fraction. C) ESI-MS spectrum of the II fraction.

A)

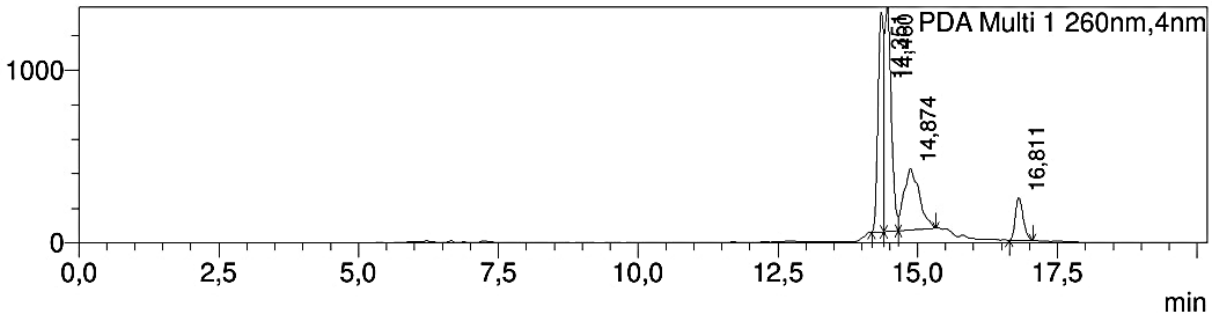

B)

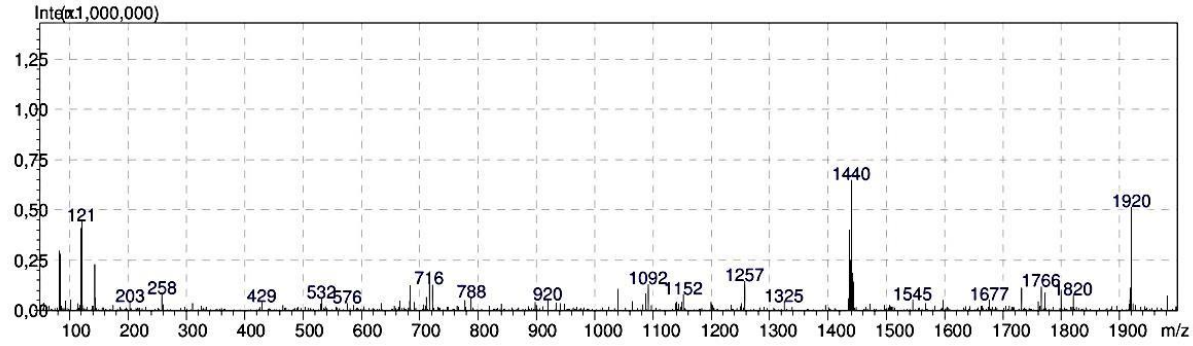

C)

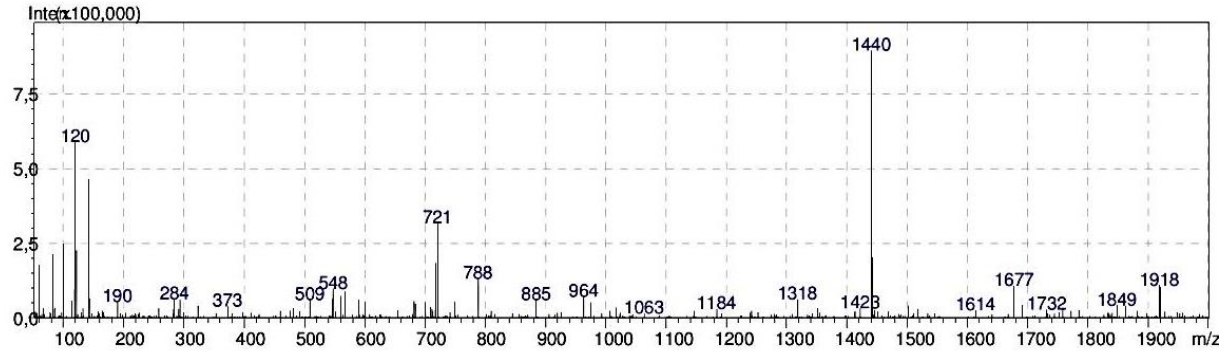

Appendix 10. ARC-1818. A) Chromatogram of the purification B) ICR-HRMS spectrum on the next page.

A)

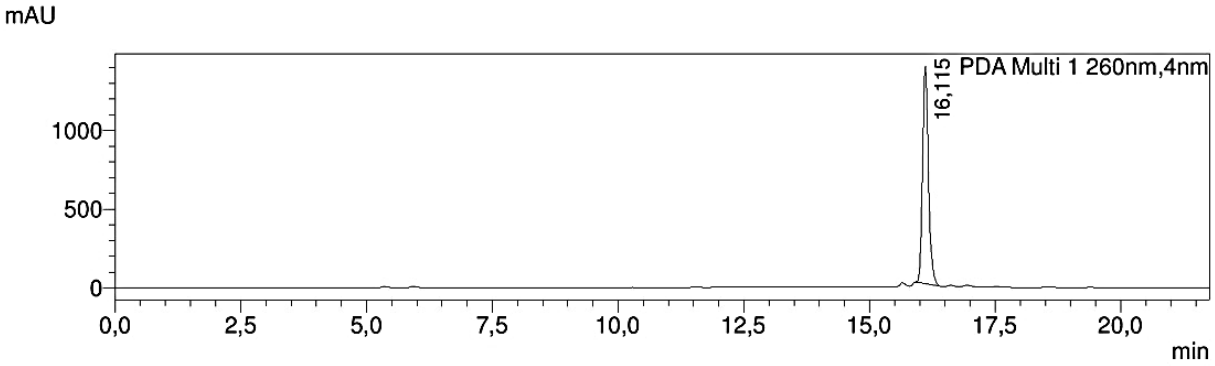

B)

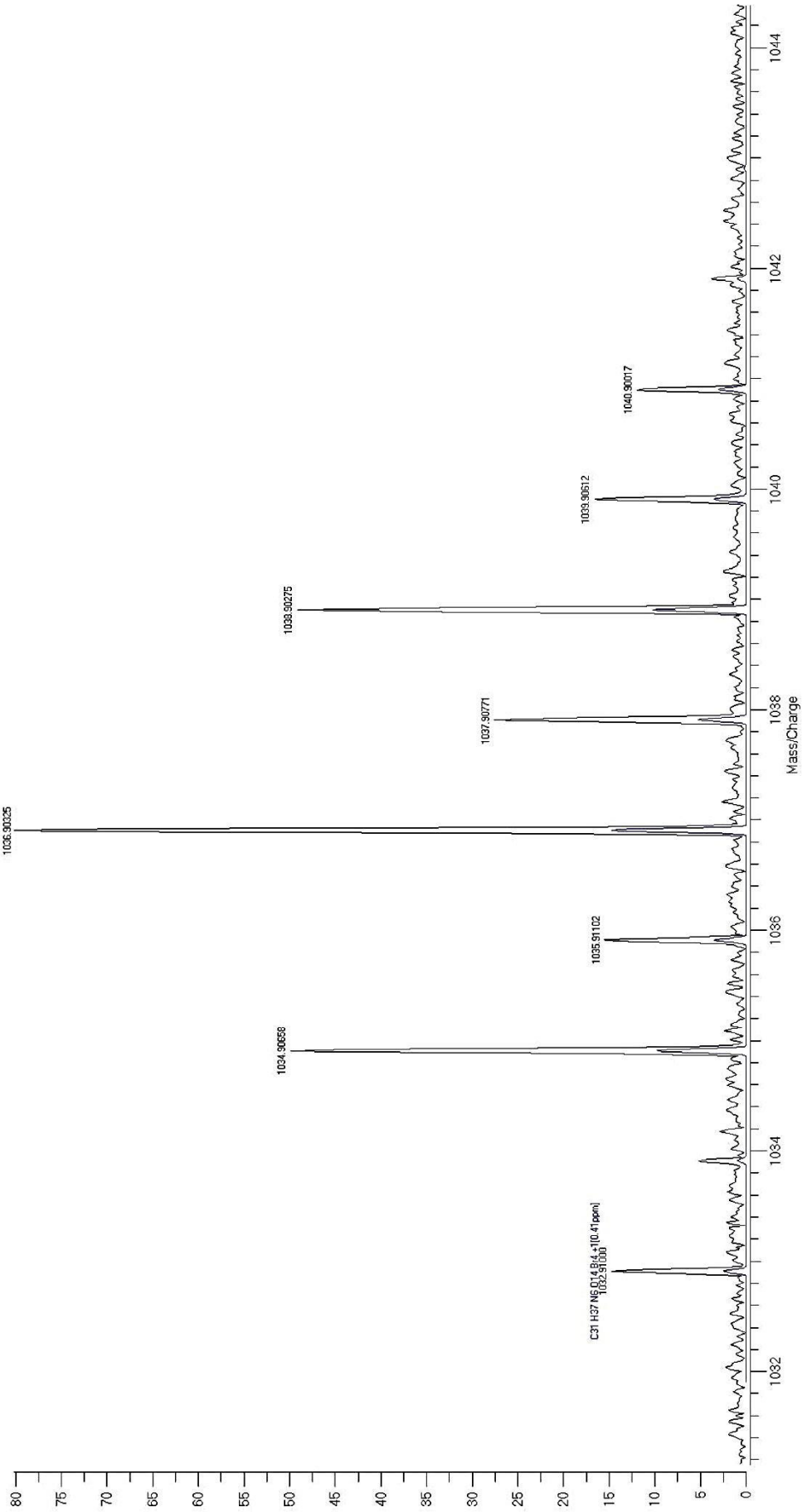
1036.90325
1038.90275
1034.90658
1037.90771
1039.90612
1040.90017
1035.91102
C31 H37 N6 O14 P4 +1 0.41 ppm
1032.91000
Mass/Charge

Appendix 11. ARC-1819 A) Chromatogram of the purification B) ESI-MS spectrum.

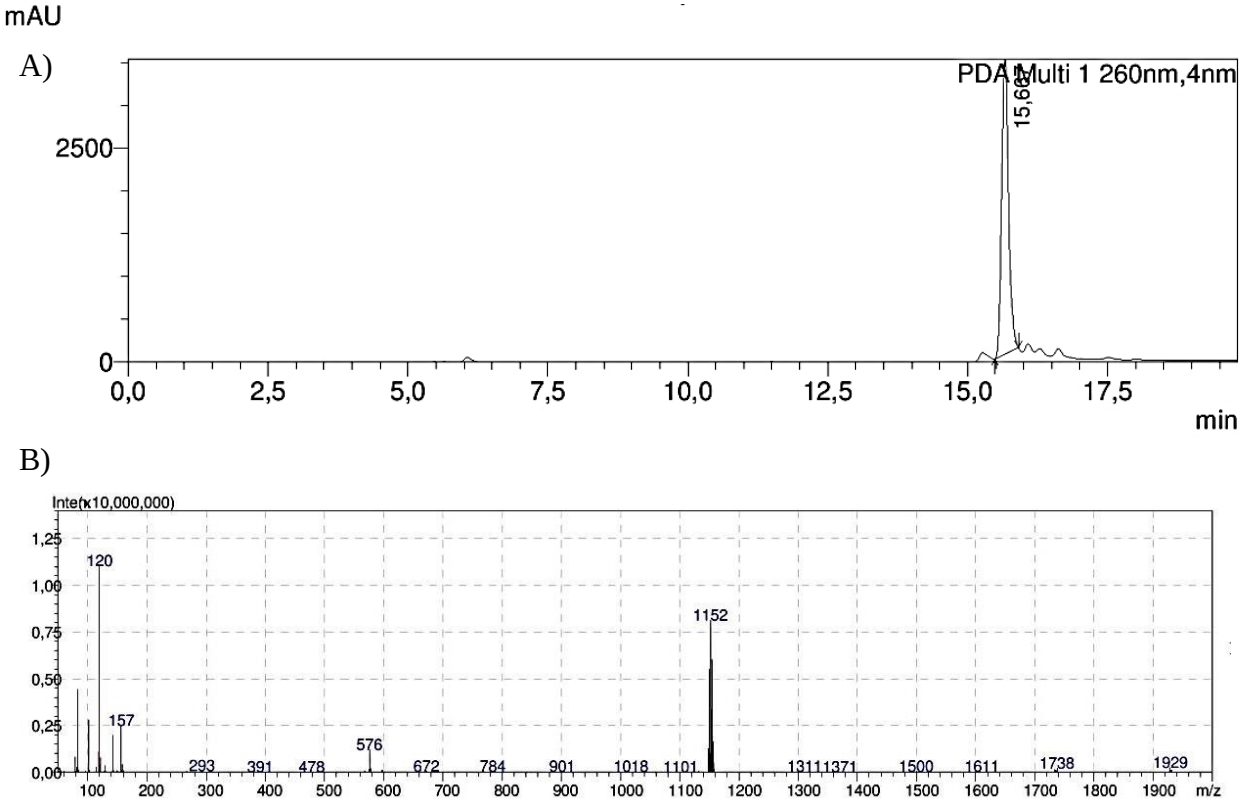

Appendix 12. ARC-1820 A) Chromatogram of the purification B) ESI-MS spectrum.

A)

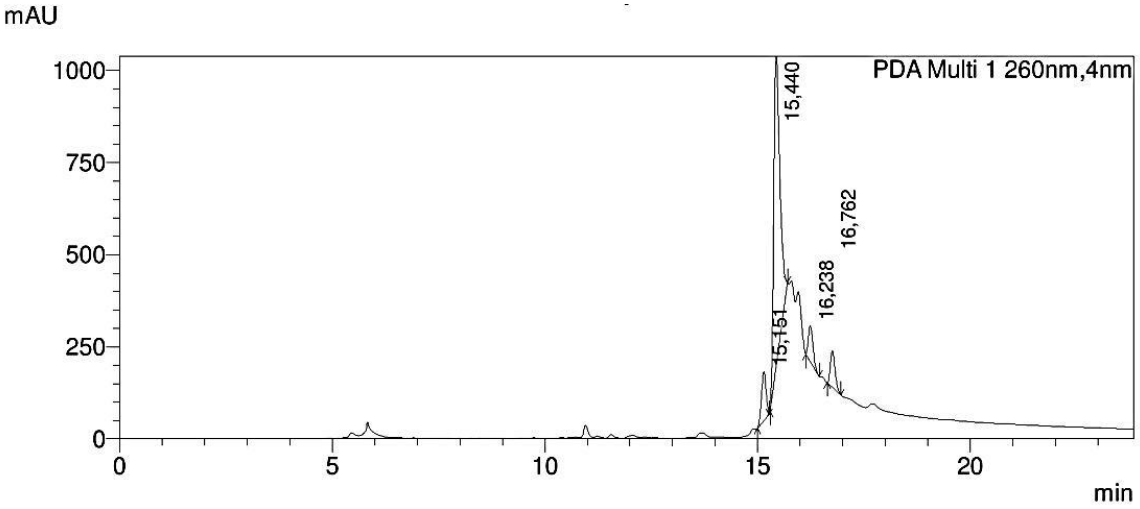

B)

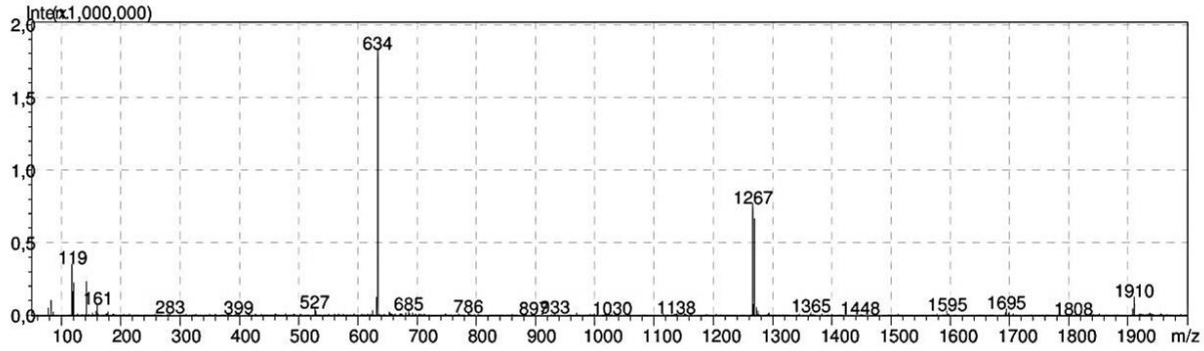

Appendix 13. ARC-1831 A) Chromatogram of the purification B) ICR-HRMS spectrum on the next page.

A)

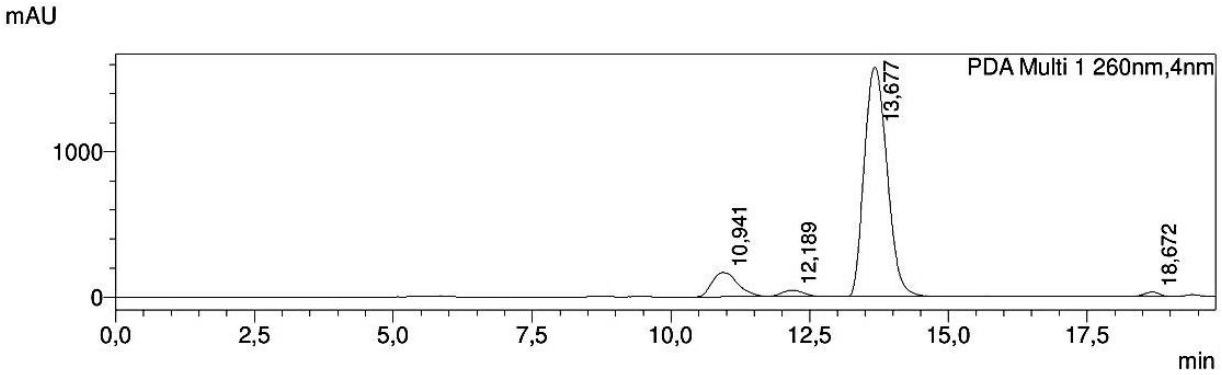

B)

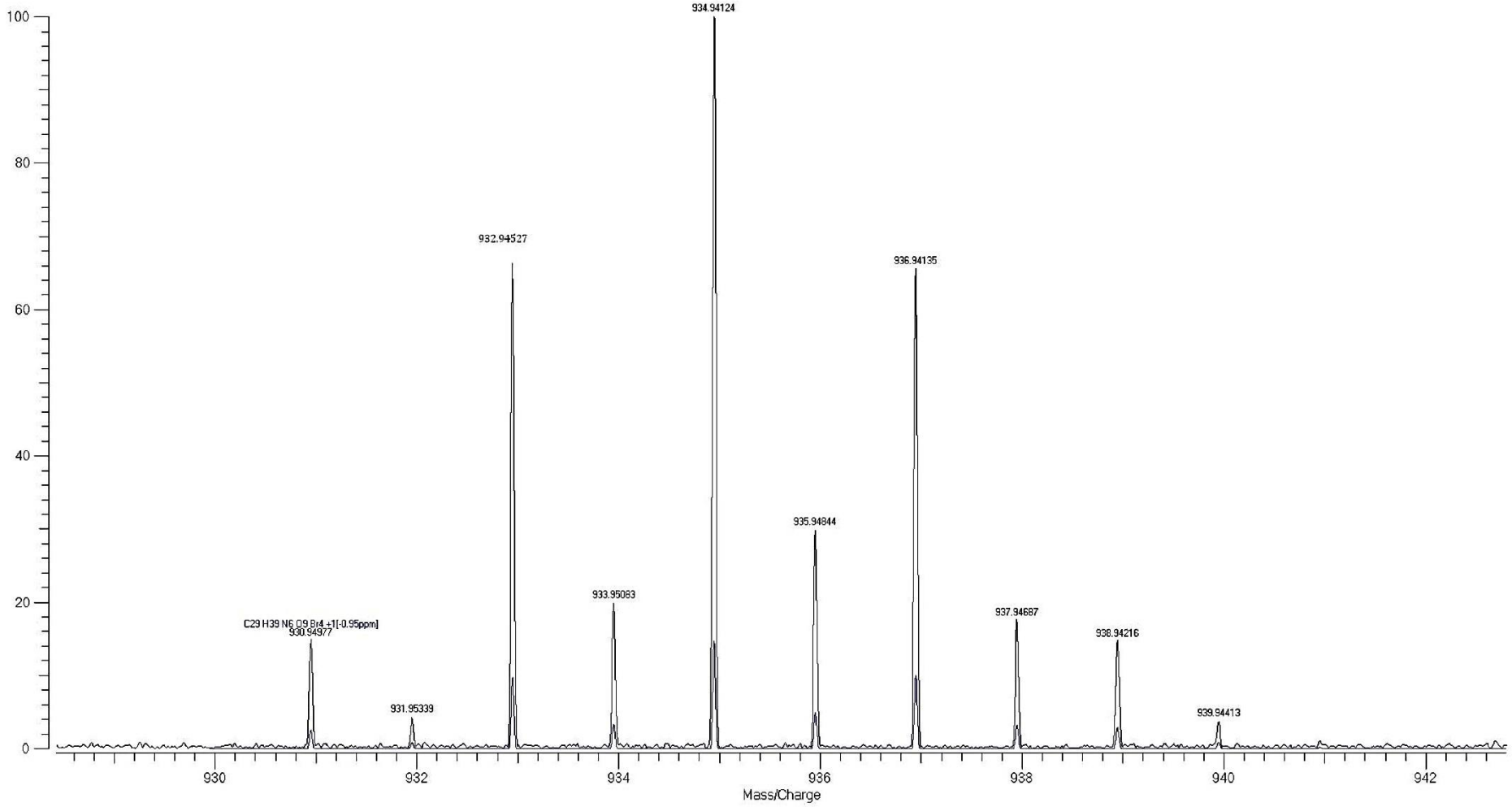
100
80
60
40
20
0
930.94977
931.95339
932.94527
933.95083
934.94124
935.94844
936.94135
937.94687
938.94216
939.94413
C29 H39 N6 O9 Br4 +1[-0.95ppm]
930
932
934
936
938
940
942
Mass/Charge

60

Appendix 14. ARC-1832 A) Chromatogram of the purification B) ESI-MS spectrum.

A)

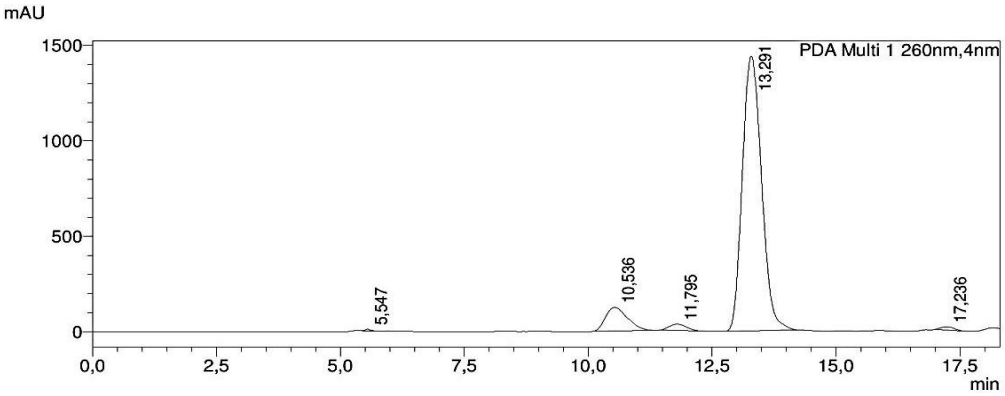

B)

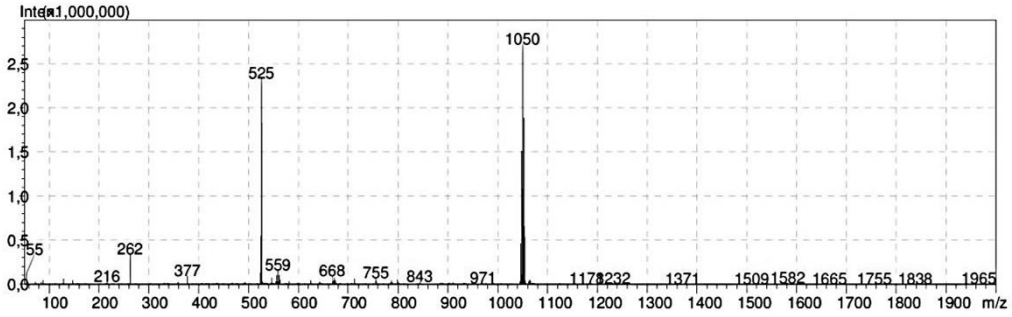

Appendix 15. ARC-1833 A) Chromatogram of the purification B) ESI-MS spectrum.

A)

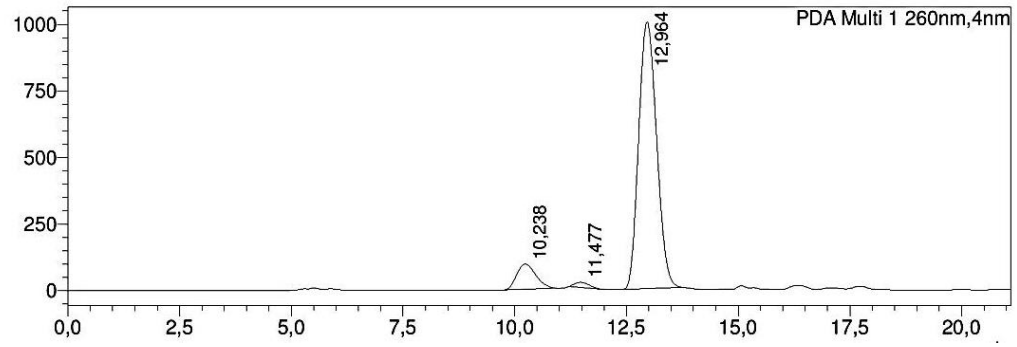

B)

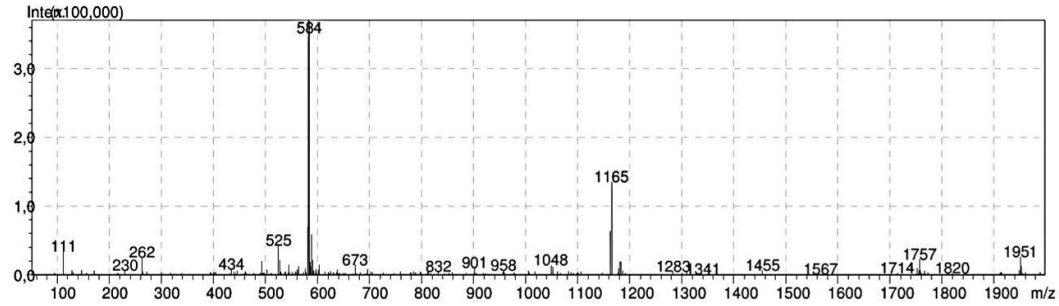

Appendix 16. ARC-1834 A) Chromatogram of the purification B) ESI-MS spectrum.

A)

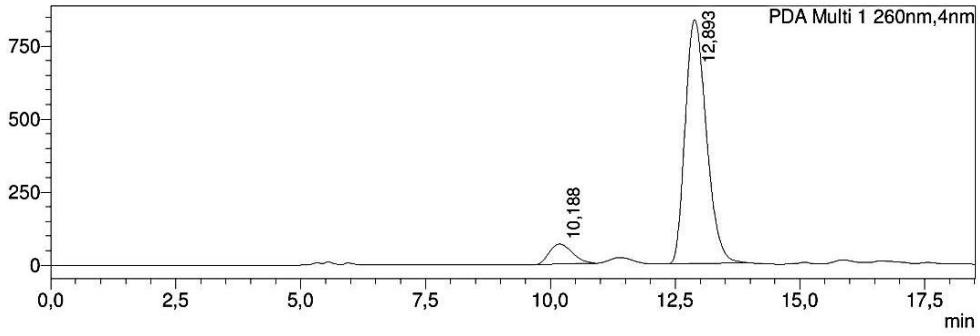

B)

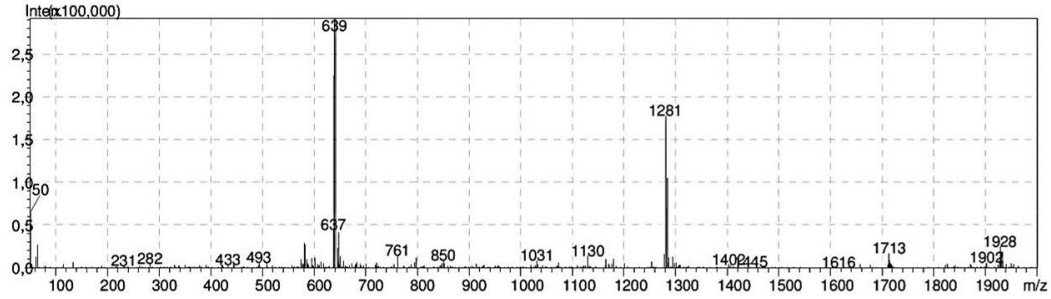

Appendix 17. ARC-1835 A) Chromatogram of the purification B) ESI-MS spectrum.

A)

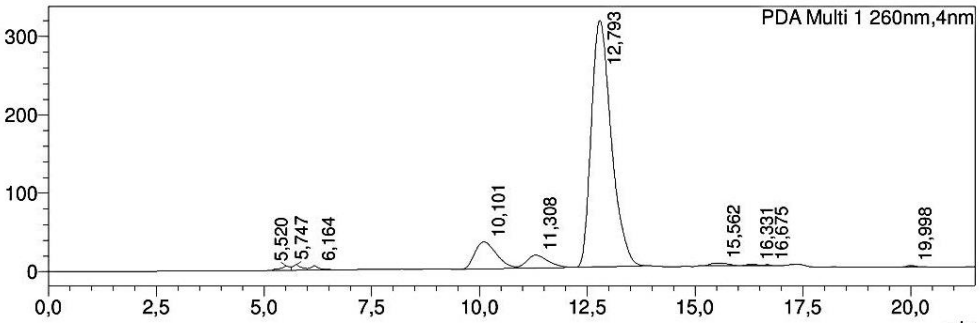

B)

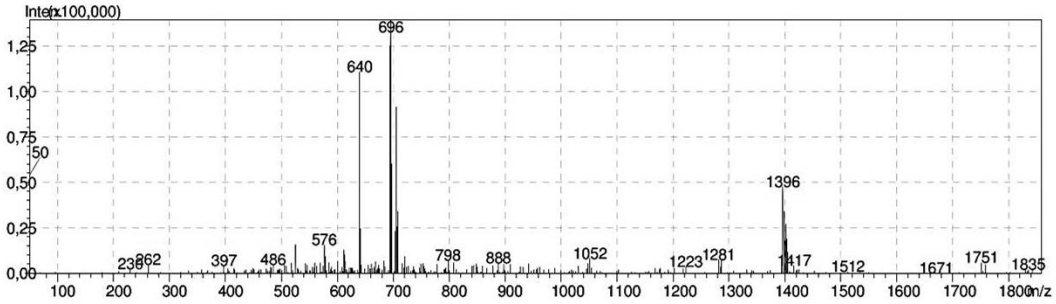

Appendix 18. ARC-1836 A) Chromatogram at 260 nm detector wavelength B) Chromatogram at 505 nm detector wavelength C) HRMS spectra.

A)

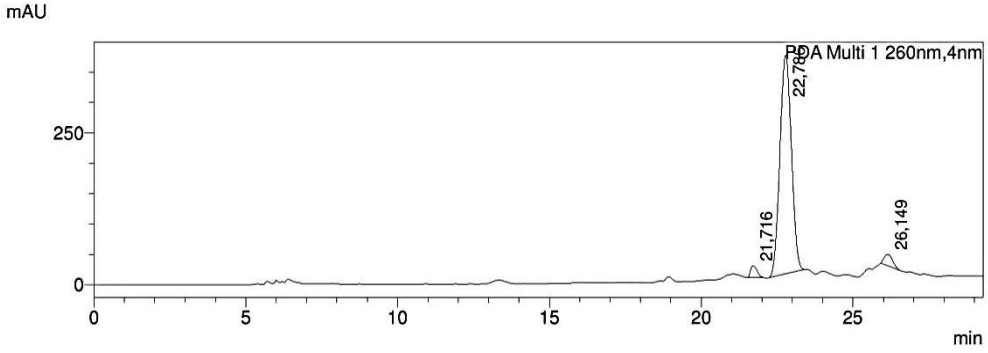

B)

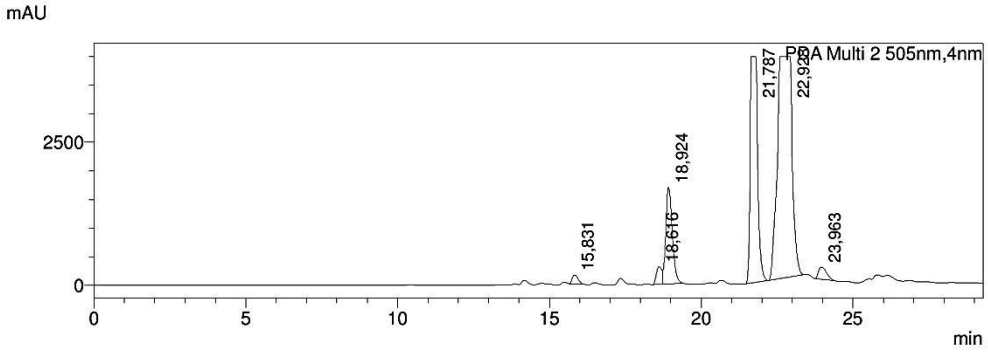

C)

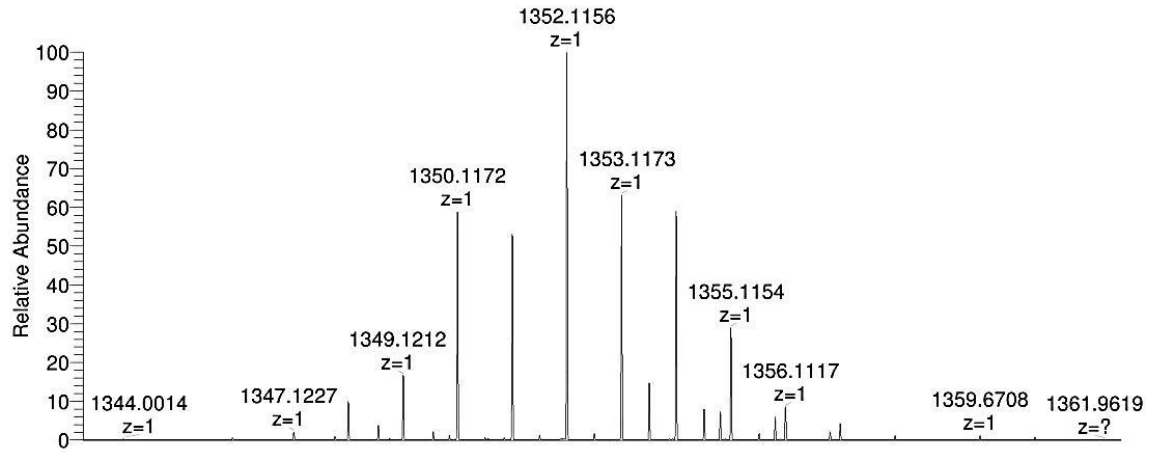

Appendix 19. ARC-1837 A) Chromatogram of the purification at 260 nm detector wavelength B) Chromatogram of the purification at 505 nm detector wavelength C) HRMS spectrum.

A)

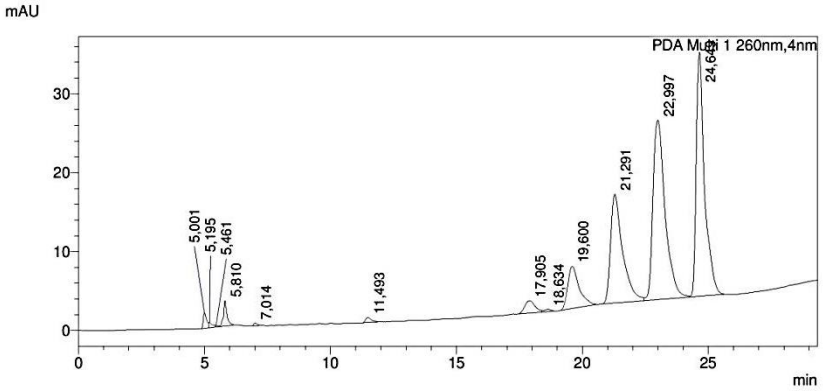

B)

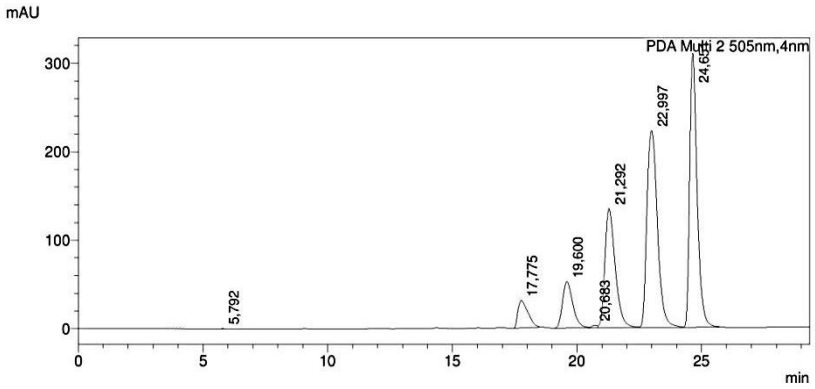

C)

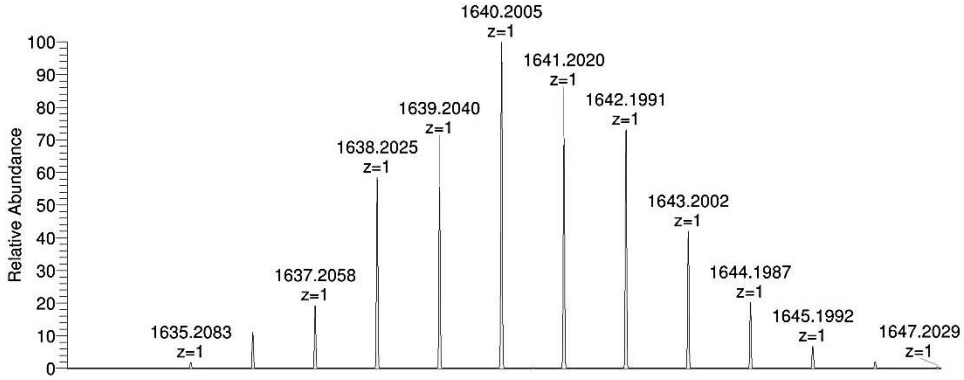

Appendix 20. ARC-1839 A) Chromatogram of the purification at 260 nm detector wavelength B) ICR-HRMS spectrum on the next page.

A)

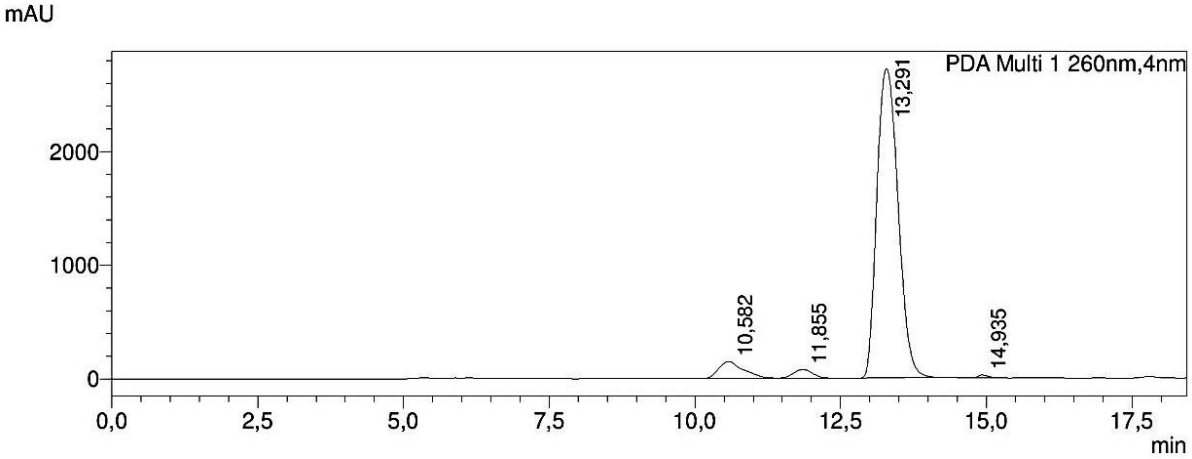

B)

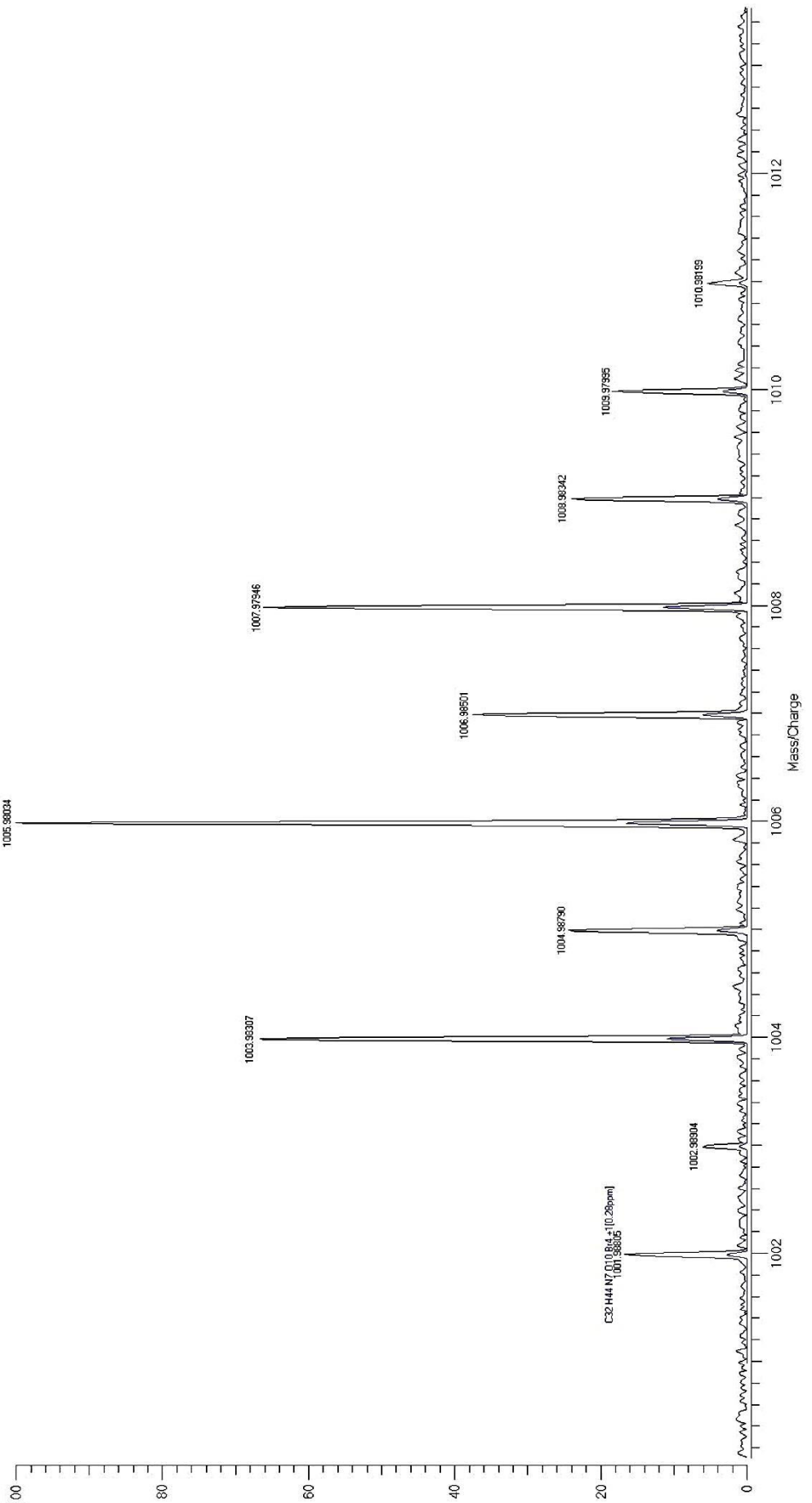
100
80
60
40
20
0
1002
1004
1006
1008
1010
1012
Mass/Charge
1001.98805
C32 H44 N7 O10 P4 -10.28ppm
1002.98304
1003.98307
1004.98790
1005.98834
1006.98501
1007.97946
1008.98342
1009.97995
1010.98199

Appendix 21. Chromatogram of the hydrolysis solution and MS spectra of every chromatographic peak (continues on the next page).

Chromatogram

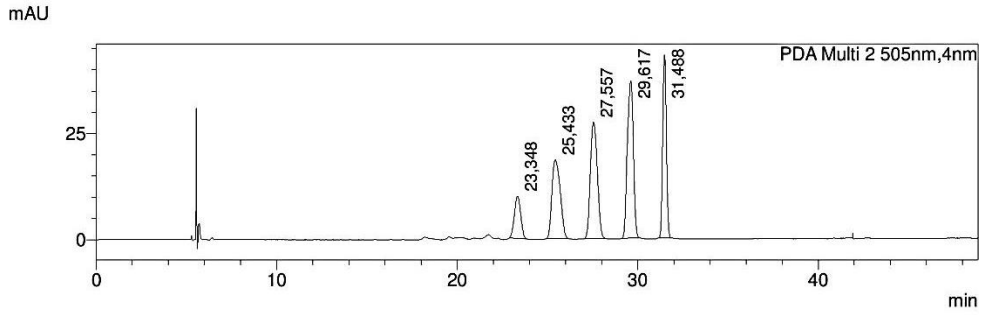

MS spectrum at 23.2 min

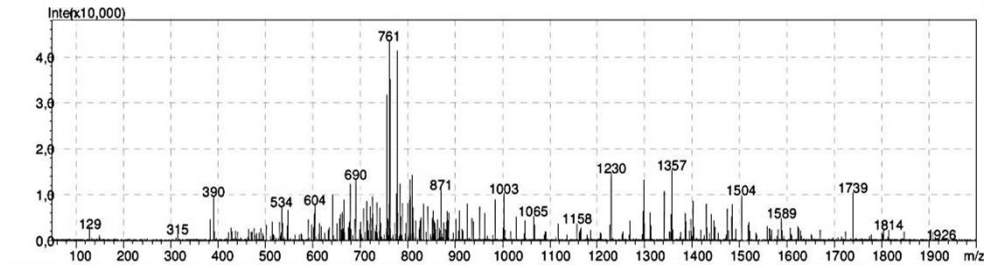

MS spectrum at 25.5 min

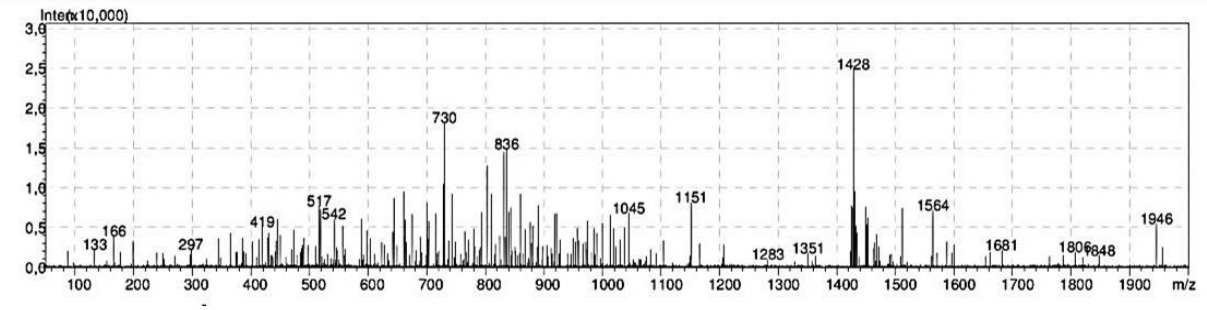

MS spectrum at 27.6 min

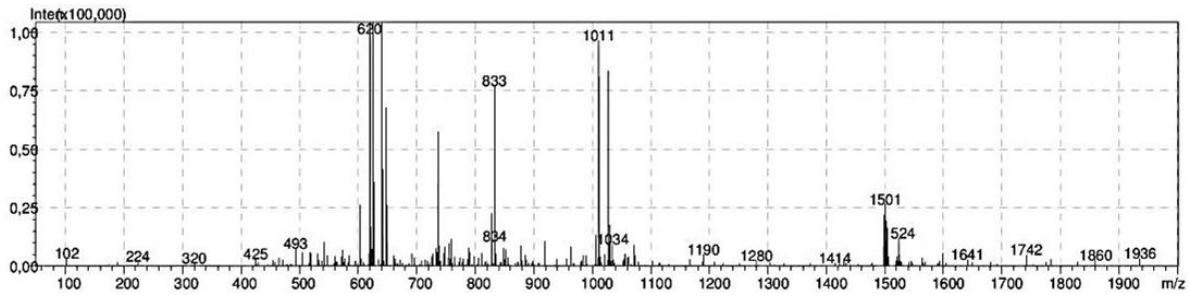

MS spectrum at 29.6 min

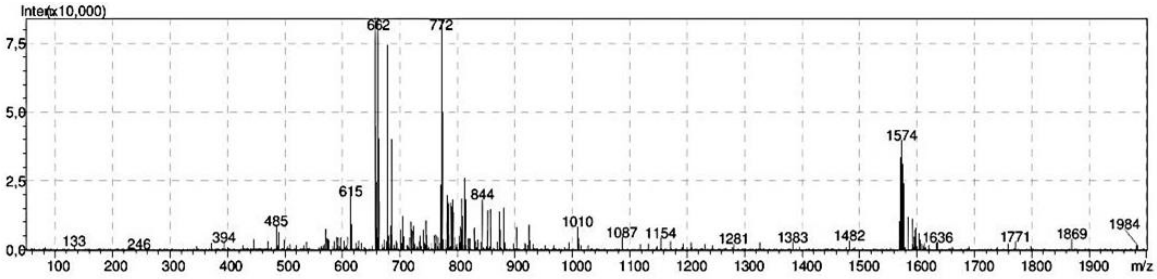

MS spectrum at 31.5 min

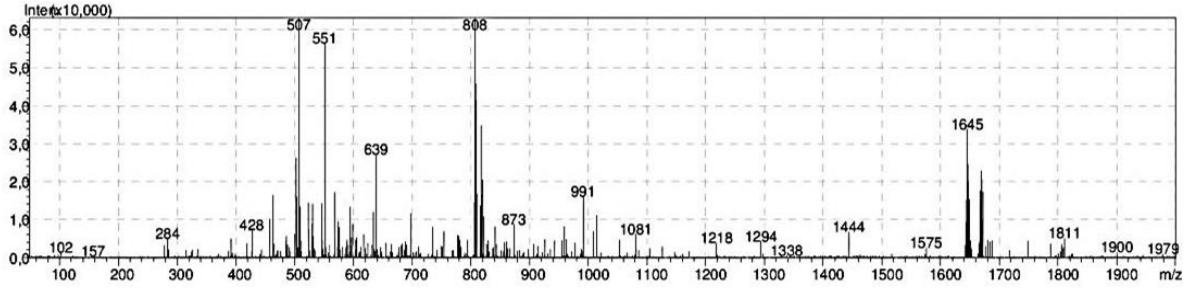

Appendix 22. Structures of ARC-1513o (**A**) and ARC-1504 (**B**).

A)

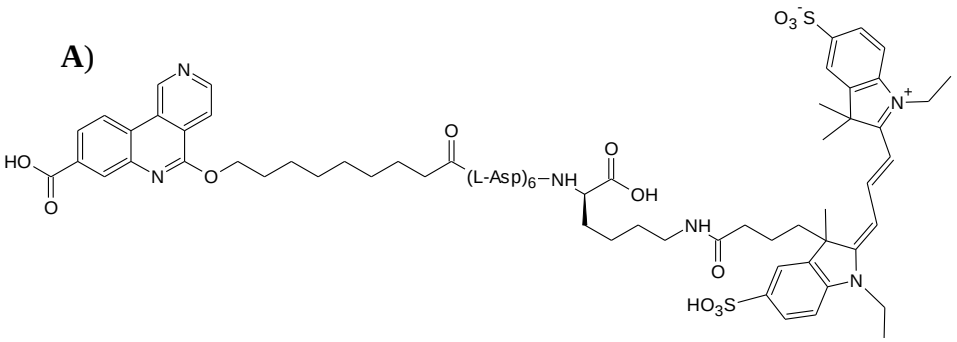

B)

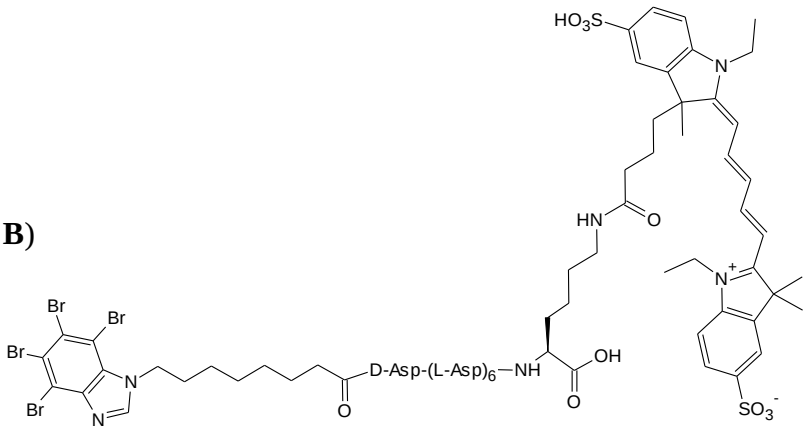

Appendix 23. Measured pIC_{50} values of inhibitors.

Compound	**pIC_{50} (SE)**
ARC-1801	-6.47 (0.03)
ARC-1802	-6.95 (0.03)
ARC-1803	-7.26 (0.10)
ARC-1818	-7.99 (0.03)
ARC-1819	-8.73 (0.10)
ARC-1820	-8.63 (0.06)
ARC-1831	-6.02 (0.05)
ARC-1832	-6.58 (0.02)
ARC-1833	-7.09 (0.03)
ARC-1834	-7.56 (0.03)
ARC-1835	-7.88 (0.03)
ARC-1839	-6.12 (0.04)

Appendix 24. Uptake of ARC-1836 and ARC-1837 by HeLa with 1 hour (A-D) and 2 hour (E-H) incubation (continues on the next page). A, E – 1 μM ARC-1836; B, F – 1 μM ARC-1837; C,G – 10 μM ARC-1836; D, H – 10 μM ARC-1837. The required intensity of the light source for ARC-1836 was 2.5 times higher than for ARC-1837 due to weaker fluorescence signal. The images are pseudocoloured.

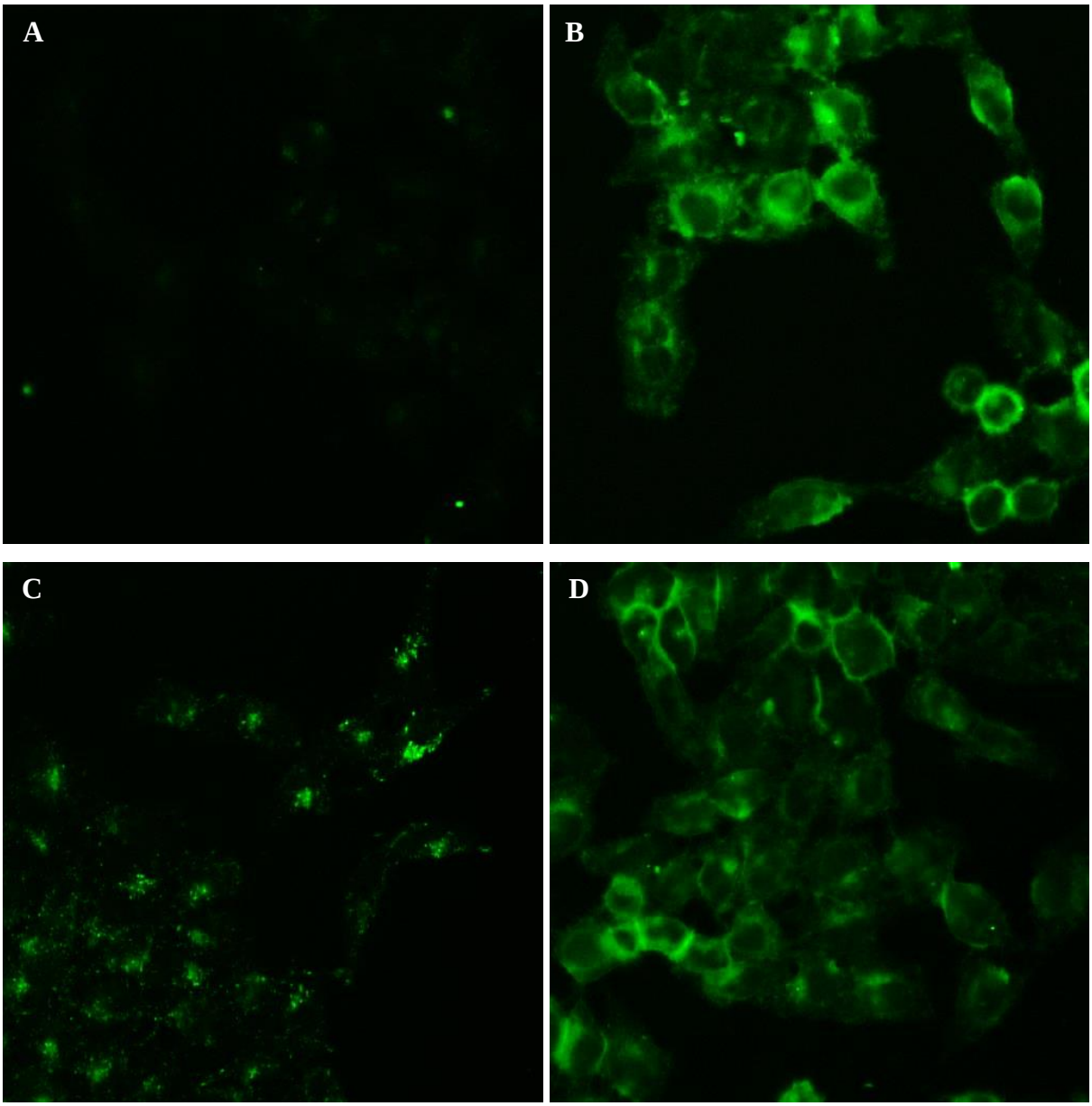

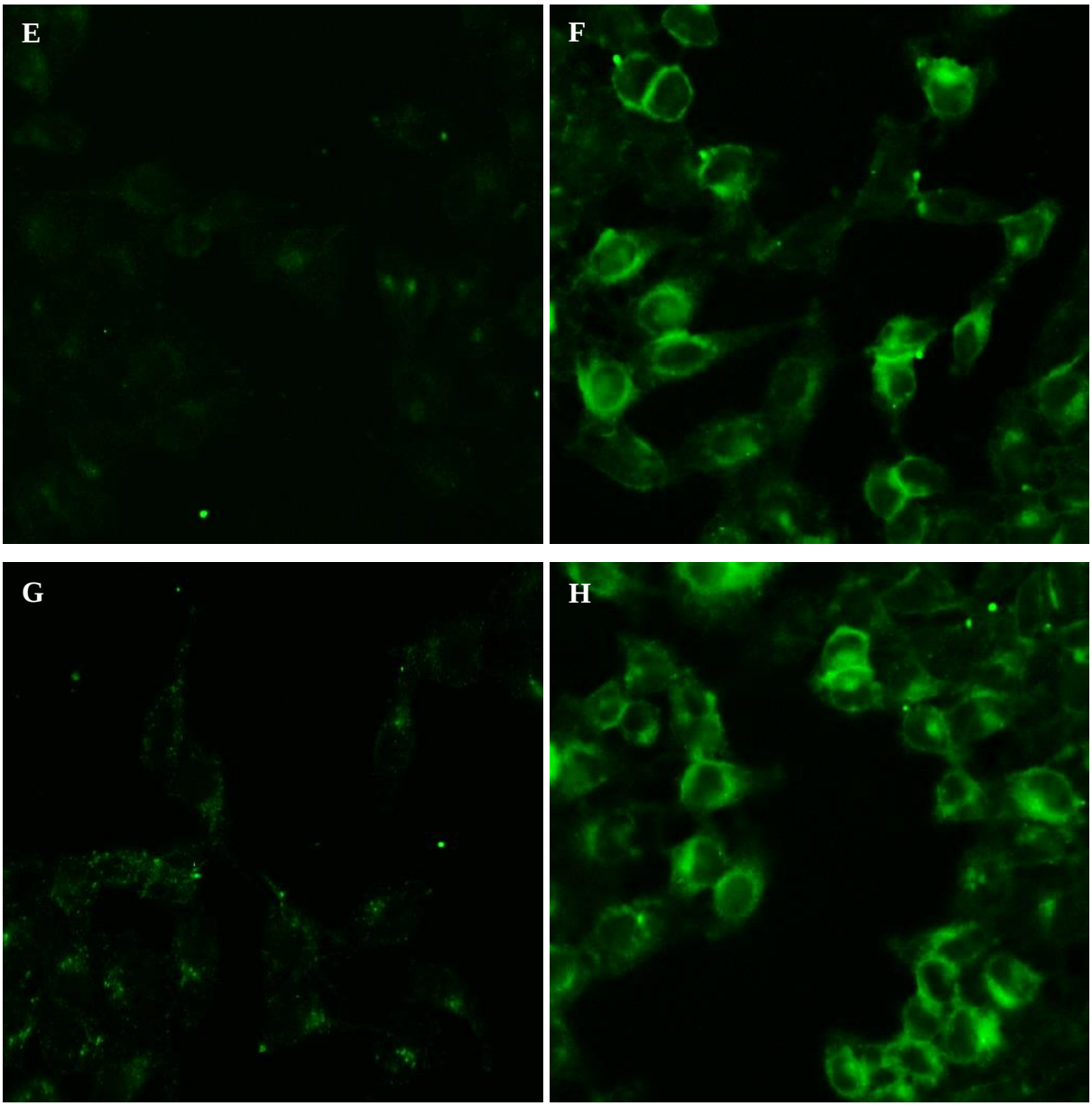
E
F
G
H

Lihtlitsents lõputöö reprodutseerimiseks ja lõputöö üldsusele kättesaadavaks tegemiseks

Mina, _____SIIRI SAAVER_____,

(*autori nimi*)

1. annan Tartu Ülikoolile tasuta loa (lihtlitsentsi) enda loodud teose
_____PRODRUG APPROACH FOR THE CELLULAR DELIVERY OF_____
_____POLYANIONIC INHIBITORS OF PROTEIN KINASE CK2_____,

(*lõputöö pealkiri*)

mille juhendaja on _____Dr Kaido Viht_____,

(*juhendaja nimi*)

1.1. reprodutseerimiseks säilitamise ja üldsusele kättesaadavaks tegemise eesmärgil, sealhulgas digitaalarhiivi DSpace-is lisamise eesmärgil kuni autoriõiguse kehtivuse tähtaja lõppemiseni;

1.2. üldsusele kättesaadavaks tegemiseks Tartu Ülikooli veebikeskkonna kaudu, sealhulgas digitaalarhiivi DSpace´i kaudu alates **02.06.2017** kuni autoriõiguse kehtivuse tähtaja lõppemiseni.

2. olen teadlik, et nimetatud õigused jäävad alles ka autorile.

3. kinnitan, et lihtlitsentsi andmisega ei rikuta teiste isikute intellektuaalomandi ega isikuandmete kaitse seadusest tulenevaid õigusi.

Tartus, **02.06.2017**